

**Mitochondrial respiratory states and rates:  
Building blocks of mitochondrial physiology  
Part 1.**

[http://www.mitoeagle.org/index.php/MitoEAGLE\\_preprint\\_2018-02-08](http://www.mitoeagle.org/index.php/MitoEAGLE_preprint_2018-02-08)

Preprint version 27 (2018-02-21)

**MitoEAGLE Network**

Corresponding author: Gnaiger E

Contributing co-authors

Aasander Frostner E, Acuna-Castroviejo D, Ahn B, Alves MG, Amati F, Aral C, Arandarčikaitė O, Bailey DM, Bastos Sant'Anna Silva AC, Battino M, Beard DA, Ben-Shachar D, Bishop D, Borutaitė V, Breton S, Brown GC, Brown RA, Buettner GR, Burtscher J, Calabria E, Cardoso LHD, Carvalho E, Casado Pinna M, Cervinkova Z, Chang SC, Chen Q, Chicco AJ, Chinopoulos C, Clementi E, Coen PM, Collin A, Collins JL, Crisóstomo L, Davis MS, De Palma C, Dias T, Distefano G, Doerrier C, Drahota Z, Duchon MR, Ehinger J, Elmer E, Endlicher R, Fell DA, Ferko M, Ferreira JCB, Filipovska A, Fisar Z, Fischer M, Fisher J, Garcia-Roves PM, Garcia-Souza LF, Genova ML, Giovarelli M, Gonzalo H, Goodpaster BH, Gorr TA, Grefte S, Han J, Harrison DK, Hellgren KT, Hernansanz-Agustin P, Holland O, Hoppel CL, Houstek J, Hunger M, Iglesias-Gonzalez J, Irving BA, Iyer S, Jackson CB, Jadiya P, Jansen-Dürr P, Jespersen NR, Jha RK, Kaambre T, Kane DA, Kappler L, Karabatsiakos A, Keijer J, Keppner G, Klingenspor M, Komlodi T, Kopitar-Jerala N, Krakovjakovic N, Kuang J, Kucera O, Labieniec-Watala M, Lai N, Laner V, Larsen TS, Lee HK, Lemieux H, Lerfall J, Lucchinetti E, MacMillan-Crow LA, Makrečka-Kuka M, Meszaros AT, Michalak S, Moiso N, Molina AJA, Montaigne D, Moore AL, Moreira BP, Mracek T, Muntane J, Muntean DM, Murray AJ, Nedergaard J, Nemeč M, Newsom S, Nozickova K, O'Gorman D, Oliveira PF, Oliveira PJ, Orynbayeva Z, Pak YK, Palmeira CM, Patel HH, Pecina P, Pereira da Silva Grilo da Silva F, Pesta D, Petit PX, Pichaud N, Pirkmajer S, Porter RK, Pranger F, Prochownik EV, Puurand M, Radenkovic F, Radi R, Reboredo P, Renner-Sattler K, Robinson MM, Rohlena J, Røslund GV, Rossiter HB, Rybacka-Mossakowska J, Saada A, Salvadego D, Scatena R, Schartner M, Scheibye-Knudsen M, Schilling JM, Schlattner U, Schoenfeld P, Schwarzer C, Scott GR, Shabalina IG, Sharma P, Sharma V, Shevchuk I, Siewiera K, Singer D, Sobotka O, Sokolova I, Spinazzi M, Stankova P, Stier A, Stocker R, Sumbalova Z, Suravajhala P, Tanaka M, Tandler B, Tepp K, Tomar D, Towheed A, Tretter L, Trifunovic A, Trivigno C, Tronstad KJ, Trougakos IP, Tyrrell DJ, Urban T, Valentine JM, Velika B, Vendelin M, Vercesi AE, Victor VM, Villena JA, Wagner BA, Ward ML, Watala C, Wei YH, Wieckowski MR, Wohlwend M, Wolff J, Wuest RCI, Zaugg K, Zaugg M, Zorzano A

Supporting co-authors:

Bakker BM, Bernardi P, Boetker HE, Borsheim E, Bouitbir J, Calbet JA, Calzia E, Chaurasia B, Coker RH, Das AM, Dubouchaud H, Durham WJ, Dyrstad SE, Engin AB, Fornaro M, Gan Z, Garlid KD, Garten A, Gourlay CW, Granata C, Haas CB, Haavik J, Haendeler J, Hand SC, Hepple RT, Hickey AJ, Hoel F, Jang DH, Kainulainen H, Khamoui AV, Koopman WJH, Kowaltowski AJ, Krajcova A, Lane N, Lenaz G, Liu J, Liu SS, Malik A, Markova M, Mazat JP, Menze MA, Methner A, Neuzil J, Oliveira MT, Pallotta ML, Parajuli N, Pettersen IKN, Porter C, Pulinilkunnil T, Ropelle ER, Salin K, Sandi C, Sazanov LA, Silber AM, Skolik R, Smenes BT, Soares FAA, Sonkar VK, Swerdlow RH, Szabo I, Thyfault JP, Vieyra A, Votion DM, Williams C, Zischka H

**Updates and discussion:**

[http://www.mitoeagle.org/index.php/MitoEAGLE\\_preprint\\_2018-02-08](http://www.mitoeagle.org/index.php/MitoEAGLE_preprint_2018-02-08)

Correspondence: Gnaiger E

Chair COST Action CA15203 MitoEAGLE – <http://www.mitoeagle.org>

Department of Visceral, Transplant and Thoracic Surgery, D. Swarovski Research  
Laboratory, Medical University of Innsbruck, Innrain 66/4, A-6020 Innsbruck, Austria

Email: erich.gnaiger@i-med.ac.at

Tel: +43 512 566796, Fax: +43 512 566796 20

**Contents****Abstract****Executive summary****1. Introduction** – Box 1: In brief: Mitochondria and Bioblasts**2. Oxidative phosphorylation and coupling states in mitochondrial preparations**

Mitochondrial preparations

*2.1. Respiratory control and coupling*

The steady-state

Specification of biochemical dose

Phosphorylation,  $P_{\gg}$ , and  $P_{\gg}/O_2$  ratio

Control and regulation

Respiratory control and response

Respiratory coupling control and ET-pathway control

Coupling

Uncoupling

*2.2. Coupling states and respiratory rates*

Respiratory capacities in coupling control states

LEAK, OXPHOS, ET, ROX

*2.3. Classical terminology for isolated mitochondria*

States 1–5

**3. Normalization: fluxes and flows***3.1. Normalization: system or sample*

Flow per system,  $I$

Extensive quantities

Size-specific quantities – Box 2: Metabolic fluxes and flows: vectorial and scalar

*3.2. Normalization for system-size: flux per chamber volume*

System-specific flux,  $J_{V,O_2}$

*3.3. Normalization: per sample*

Sample concentration,  $C_{mX}$

Mass-specific flux,  $J_{O_2/mX}$

Number concentration,  $C_{NX}$

Flow per object,  $I_{O_2/X}$

*3.4. Normalization for mitochondrial content*

Mitochondrial concentration,  $C_{mtE}$ , and mitochondrial markers

Mitochondria-specific flux,  $J_{O_2/mtE}$

*3.5. Evaluation of mitochondrial markers**3.6. Conversion: units***4. Conclusions** – Box 3: Mitochondrial and cell respiration**5. References**

102 **Abstract** As the knowledge base and importance of mitochondrial physiology to human health  
103 expand, the necessity for harmonizing nomenclature concerning mitochondrial respiratory  
104 states and rates has become increasingly apparent. Clarity of concept and consistency of  
105 nomenclature are key trademarks of a research field. These trademarks facilitate effective  
106 transdisciplinary communication, education, and ultimately further discovery. Peter Mitchell's  
107 chemiosmotic theory establishes the mechanism of energy transformation and coupling in  
108 oxidative phosphorylation. The unifying concept of the protonmotive force provides the  
109 framework for developing a consistent theory and nomenclature for mitochondrial physiology  
110 and bioenergetics. Herein, we follow IUPAC guidelines on general terms of physical chemistry,  
111 extended by considerations on open systems and irreversible thermodynamics. We align the  
112 nomenclature and symbols of classical bioenergetics with a concept-driven constructive  
113 terminology to express the meaning of each quantity clearly and consistently. In this position  
114 statement, in the frame of COST Action MitoEAGLE, we endeavour to provide a balanced  
115 view on mitochondrial respiratory control and a critical discussion on reporting data of  
116 mitochondrial respiration in terms of metabolic flows and fluxes. Uniform standards for  
117 evaluation of respiratory states and rates will ultimately support the development of databases  
118 of mitochondrial respiratory function in species, tissues, and cells.

119

120 *Keywords:* Mitochondrial respiratory control, coupling control, mitochondrial  
121 preparations, protonmotive force, oxidative phosphorylation, OXPHOS, efficiency, electron  
122 transfer, ET; proton leak, LEAK, residual oxygen consumption, ROX, State 2, State 3, State 4,  
123 normalization, flow, flux, O<sub>2</sub>

124

125

126

127

---

## 127 **Executive summary**

128

129

130

131

132

133

134

135

136

137

138

139

140

141

142

143

144

145

146

147

148

149

150

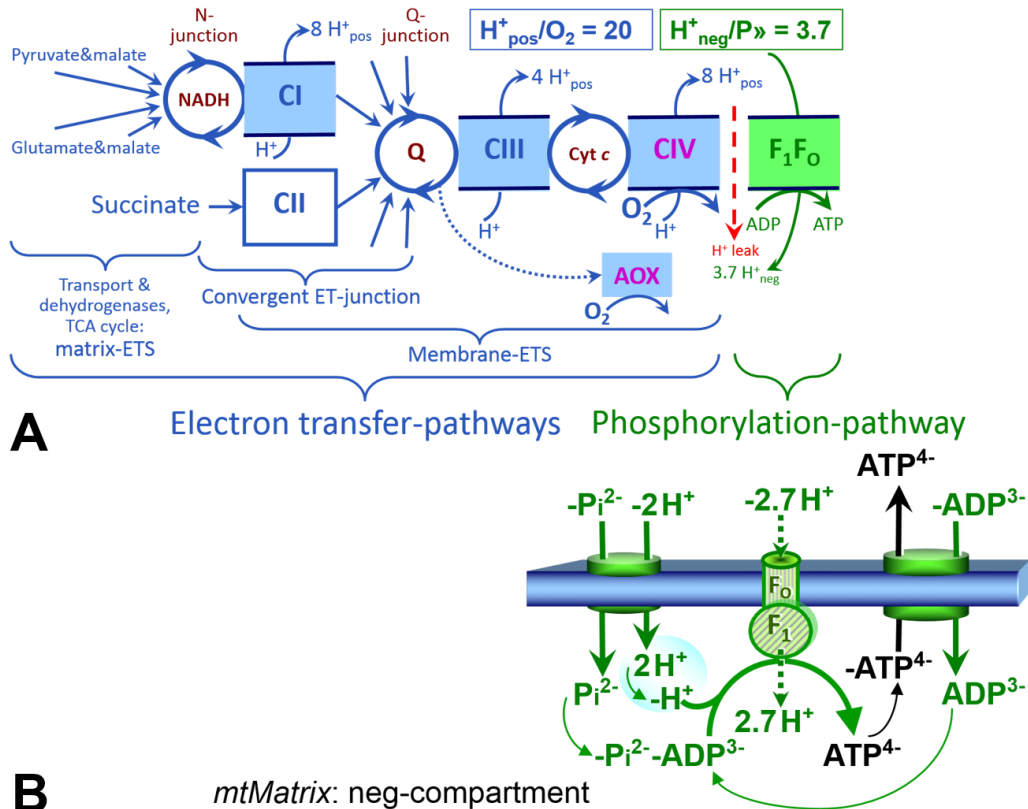
151

152

1. In view of broad implications on health care, mitochondrial researchers face an increasing responsibility to disseminate their fundamental knowledge and novel discoveries to a wide range of stakeholders and scientists beyond the group of specialists. This requires implementation of a commonly accepted terminology within the discipline and standardization in the translational context. Authors, reviewers, journal editors, and lecturers are challenged to collaborate with the aim to harmonize the nomenclature in the growing field of mitochondrial physiology and bioenergetics.
2. Aerobic energy metabolism in mammalian mitochondria depends on the coupling of phosphorylation (ADP → ATP) to O<sub>2</sub> flux in catabolic reactions. In this process of oxidative phosphorylation, coupling is mediated by translocation of protons through respiratory proton pumps operating across the inner mitochondrial membrane and generating or utilizing the protonmotive force measured between the mitochondrial matrix and intermembrane compartment. Compartmental coupling thus distinguishes vectorial oxidative phosphorylation from fermentation as the counterpart of cellular core energy metabolism.
3. To exclude fermentation and other cytosolic interactions from exerting an effect on mitochondrial metabolism, the barrier function of the plasma membrane must be disrupted. Selective removal or permeabilization of the plasma membrane yields mitochondrial preparations—including isolated mitochondria, tissue and cellular preparations—with structural and functional integrity. Then extra-mitochondrial concentrations of fuel substrates transported into the mitochondrial matrix, ADP, ATP, inorganic phosphate, and cations including H<sup>+</sup> can be controlled to determine mitochondrial function under a set of conditions defined as coupling control states.

153  
154  
155  
156  
157

A concept-driven terminology of bioenergetics incorporates in its terms and symbols explicitly information on the nature of respiratory states, that makes the technical terms readily recognized and easy to understand.



158  
159  
160  
161  
162  
163  
164  
165  
166  
167  
168  
169  
170  
171  
172  
173  
174  
175  
176  
177  
178  
179

**Fig. 1. The oxidative phosphorylation (OXPHOS) system.** (A) The mitochondrial electron transfer system (ETS) is fuelled by diffusion and transport of substrates across the mtOM and mtIM and consists of the matrix-ETS and membrane-ETS. ET-pathways are coupled to the phosphorylation-pathway. ET-pathways converge at the N-junction and Q-junction. Additional arrows indicate electron entry into the Q-junction through electron transferring flavoprotein, glycerophosphate dehydrogenase, dihydro-orotate dehydrogenase, choline dehydrogenase, and sulfide-ubiquinone oxidoreductase. The dotted arrow indicates the branched pathway of oxygen consumption by alternative quinol oxidase (AOX). The  $H^+_{pos}/O_2$  ratio is the outward proton flux from the matrix space to the positively (pos) charged compartment, divided by catabolic  $O_2$  flux in the NADH-pathway. The  $H^+_{neg}/P \gg$  ratio is the inward proton flux from the inter-membrane space to the negatively (neg) charged matrix space, divided by the flux of phosphorylation of ADP to ATP (Eq. 1). These are not fixed stoichiometries due to ion leaks and proton slip. (B) Phosphorylation-pathway catalyzed by the proton pump F<sub>1</sub>F<sub>0</sub>-ATPase (F-ATPase, ATP synthase), adenine nucleotide translocase, and inorganic phosphate transporter. The  $H^+_{neg}/P \gg$  stoichiometry is the sum of the coupling stoichiometry in the F-ATPase reaction ( $-2.7 H^+_{pos}$  from the positive intermembrane space,  $2.7 H^+_{neg}$  to the matrix, *i.e.*, the negative compartment) and the proton balance in the translocation of ADP<sup>2-</sup>, ATP<sup>3-</sup> and Pi<sup>2-</sup>. Modified from (A) Lemieux *et al.* (2017) and (B) Gnaiger (2014).

- 180 4. Mitochondrial coupling states are defined according to the control of respiratory oxygen  
 181 flux by the protonmotive force. Capacities of oxidative phosphorylation and  
 182 electron transfer capacities are measured at kinetically saturating concentrations of  
 183 fuel substrates, ADP and inorganic phosphate, or at optimal uncoupler  
 184 concentrations, respectively. Respiratory capacities are a measure of the upper  
 185 bound of the rates of respiration, providing reference values for the diagnosis of  
 186 health and disease, and for evaluation of the effects of **E**volutionary background,  
 187 **A**ge, **G**ender and sex, **L**ifestyle and **E**nvironment (EAGLE).
- 188 5. Some degree of uncoupling is a characteristic of energy-transformations across  
 189 membranes. Uncoupling is caused by a variety of physiological, pathological,  
 190 toxicological, pharmacological and environmental conditions that exert an  
 191 influence not only on the proton leak and cation cycling, but also on proton slip  
 192 within the proton pumps and the structural integrity of the mitochondria. A more  
 193 loosely coupled state is induced by stimulation of mitochondrial superoxide  
 194 formation and the bypass of proton pumps. In addition, uncoupling by application  
 195 of protonophores represents an experimental intervention for the transition from a  
 196 well-coupled to the noncoupled state of mitochondrial respiration.
- 197 6. Respiratory oxygen consumption rates have to be carefully normalized to enable meta-  
 198 analytic studies beyond the specific question of a particular experiment. Therefore,  
 199 all raw data should be published in a supplemental table or open access data  
 200 repository. Normalization of rates for the volume of the experimental chamber (the  
 201 measuring system) is distinguished from normalization for (1) the volume or mass  
 202 of the experimental sample, (2) the number of objects (cells, organisms), and (3)  
 203 the concentration of mitochondrial markers in the chamber.
- 204 7. The consistent use of terms and symbols discussed in this MitoEAGLE position  
 205 statement will facilitate transdisciplinary communication and support further  
 206 developments of a database on bioenergetics and mitochondrial physiology. The  
 207 present considerations are focused on studies with mitochondrial preparations.  
 208 These will be extended in a series of reports on pathway control of mitochondrial  
 209 respiration, the protonmotive force, respiratory states in intact cells, and  
 210 harmonization of experimental procedures.

---

### 215 **Box 1: In brief – Mitochondria and Bioblasts**

216 **Mitochondria** are the oxygen-consuming electrochemical generators evolved from  
 217 endosymbiotic bacteria (Margulis 1970; Lane 2005). They were described by Richard Altmann  
 218 (1894) as ‘bioblasts’, which include not only the mitochondria as presently defined, but also  
 219 symbiotic and free-living bacteria. The word ‘mitochondria’ (Greek mitos: thread; chondros:  
 220 granule) was introduced by Carl Benda (1898).

221 Mitochondrial dysfunction is associated with a wide variety of genetic and degenerative  
 222 diseases. Robust mitochondrial function is supported by physical exercise and caloric balance,  
 223 and is central for sustained metabolic health throughout life. Therefore, a more consistent  
 224 presentation of mitochondrial physiology will improve our understanding of the etiology of  
 225 disease, the diagnostic repertoire of mitochondrial medicine, with a focus on protective  
 226 medicine, lifestyle and healthy aging.

227 We now recognize mitochondria as dynamic organelles with a double membrane that are  
 228 contained within eukaryotic cells. The mitochondrial inner membrane (mtIM) shows dynamic  
 229 tubular to disk-shaped cristae that separate the mitochondrial matrix, *i.e.*, the negatively charged  
 230



231 internal mitochondrial compartment, and the intermembrane space; the latter being positively  
232 charged and enclosed by the mitochondrial outer membrane (mtOM). The mtIM contains the  
233 non-bilayer phospholipid cardiolipin, which is not present in any other eukaryotic cellular  
234 membrane. Cardiolipin promotes the formation of respiratory supercomplexes, which are  
235 supramolecular assemblies based upon specific, though dynamic, interactions between  
236 individual respiratory complexes (Greggio *et al.* 2017; Lenaz *et al.* 2017). Membrane fluidity  
237 exerts an influence on functional properties of proteins incorporated in the membranes  
238 (Waczulikova *et al.* 2007).

239 Mitochondria are the structural and functional elements of cell respiration. Cell  
240 respiration is the reduction of oxygen by electron transfer coupled to electrochemical proton  
241 translocation across the mtIM. In the process of oxidative phosphorylation (OXPHOS), the  
242 catabolic reaction of oxygen consumption is electrochemically coupled to the transformation of  
243 energy in the form of adenosine triphosphate (ATP; Mitchell 1961, 2011). Mitochondria are the  
244 powerhouses of the cell which contain the machinery of the OXPHOS-pathways, including  
245 transmembrane respiratory complexes—proton pumps with FMN, Fe-S and cytochrome *b*, *c*,  
246 *aa<sub>3</sub>* redox systems); alternative dehydrogenases and oxidases; the coenzyme ubiquinone (Q);  
247 F-ATPase or ATP synthase; the enzymes of the tricarboxylic acid cycle and fatty acid oxidation;  
248 transporters of ions, metabolites and co-factors; and mitochondrial kinases related to energy  
249 transfer pathways. The mitochondrial proteome comprises over 1,200 proteins (Calvo *et al.*  
250 2015; 2017), mostly encoded by nuclear DNA (nDNA), with a variety of functions, many of  
251 which are relatively well known (*e.g.*, apoptosis-regulating proteins), while others are still under  
252 investigation, or need to be identified (*e.g.*, alanine transporter).

253 There is a constant crosstalk between mitochondria and the other cellular components.  
254 The crosstalk between mitochondria and endoplasmic reticulum is involved in the regulation of  
255 calcium homeostasis, cell division, autophagy, differentiation, anti-viral signaling (Murley and  
256 Nunnari 2016). Cellular mitostasis is maintained through regulation at both the transcriptional  
257 and post-translational level, through cell signalling including proteostatic (*e.g.*, the ubiquitin-  
258 proteasome and autophagy-lysosome pathways), and genome stability modules throughout the  
259 cell cycle or even cell death, contributing to homeostatic regulation in response to varying  
260 energy demands and stress (Quiros *et al.* 2016). In addition to mitochondrial movement along  
261 microtubules, mitochondrial morphology can change in response to energy requirements of the  
262 cell via processes known as fusion and fission, through which mitochondria communicate  
263 within a network, and in response to intracellular stress factors causing swelling and ultimately  
264 permeability transition.

265 Mitochondria typically maintain several copies of their own genome known as  
266 mitochondrial DNA (mtDNA; hundred to thousands per cell; Cummins 1998), which is  
267 maternally inherited. One exception to strictly maternal inheritance in animals is found in  
268 bivalves (Breton *et al.* 2007; White *et al.* 2008). mtDNA is 16.5 kB in length, contains 13  
269 protein-coding genes for subunits of the transmembrane respiratory Complexes CI, CIII, CIV  
270 and F-ATPase, and also encodes 22 tRNAs and the mitochondrial 16S and 12S rRNA.  
271 Additional gene content is encoded in the mitochondrial genome, *e.g.*, microRNAs, piRNA,  
272 smithRNAs, repeat associated RNA, and even additional proteins, *e.g.*, the small peptides  
273 humanin and MOTS-c (Duarte *et al.* 2014; Lee *et al.* 2015; Cobb *et al.* 2016). The mitochondrial  
274 genome is regulated and supplemented by nuclear-encoded mitochondrial targeted proteins.

275 Abbreviation: mt, as generally used in mtDNA. Mitochondrion is singular and  
276 mitochondria is plural.

277 *‘For the physiologist, mitochondria afforded the first opportunity for an experimental*  
278 *approach to structure-function relationships, in particular those involved in active transport,*  
279 *vectorial metabolism, and metabolic control mechanisms on a subcellular level’* (Ernster and  
280 Schatz 1981).

281

---

## 282 1. Introduction

283

284 Mitochondria are the powerhouses of the cell with numerous physiological, molecular,  
285 and genetic functions (**Box 1**). Every study of mitochondrial health and disease is faced with  
286 **E**volution, **A**ge, **G**ender and sex, **L**ifestyle, and **E**nvironment (EAGLE) as essential background  
287 conditions intrinsic to the individual patient or subject, cohort, species, tissue and to some extent  
288 even cell line. As a large and coordinated group of laboratories and researchers, the mission of  
289 the global MitoEAGLE Network is to generate the necessary scale, type, and quality of  
290 consistent data sets and conditions to address this intrinsic complexity. Harmonization of  
291 experimental protocols and implementation of a quality control and data management system  
292 are required to interrelate results gathered across a spectrum of studies and to generate a  
293 rigorously monitored database focused on mitochondrial respiratory function. In this way,  
294 researchers within the same and across different disciplines will be positioned to compare  
295 findings across traditions and generations to an agreed upon set of clearly defined and accepted  
296 international standards.

297 Reliability and comparability of quantitative results depend on the accuracy of  
298 measurements under strictly-defined conditions. A conceptual framework is required to warrant  
299 meaningful interpretation and comparability of experimental outcomes carried out by research  
300 groups at different institutes. With an emphasis on quality of research, collected data can be  
301 useful far beyond the specific question of a particular experiment. Enabling meta-analytic  
302 studies is the most economic way of providing robust answers to biological questions (Cooper  
303 *et al.* 2009). Vague or ambiguous jargon can lead to confusion and may relegate valuable  
304 signals to wasteful noise. For this reason, measured values must be expressed in standard units  
305 for each parameter used to define mitochondrial respiratory function. Harmonization of  
306 nomenclature and definition of technical terms are essential to improve the awareness of the  
307 intricate meaning of current and past scientific vocabulary, for documentation and integration  
308 into databases in general, and quantitative modelling in particular (Beard 2005). The focus on  
309 coupling states and fluxes through metabolic pathways of aerobic energy transformation in  
310 mitochondrial preparations is a first step in the attempt to generate a conceptually-oriented  
311 nomenclature in bioenergetics and mitochondrial physiology. Coupling states of intact cells,  
312 the protonmotive force, and respiratory control by fuel substrates and specific inhibitors of  
313 respiratory enzymes will be reviewed in subsequent communications.

314

315

## 316 2. Oxidative phosphorylation and coupling states in mitochondrial preparations

317 *‘Every professional group develops its own technical jargon for talking about matters of*  
318 *critical concern ... People who know a word can share that idea with other members of*  
319 *their group, and a shared vocabulary is part of the glue that holds people together and*  
320 *allows them to create a shared culture’ (Miller 1991).*

321

322 **Mitochondrial preparations** are defined as either isolated mitochondria, or tissue and  
323 cellular preparations in which the barrier function of the plasma membrane is disrupted. Since  
324 this entails the loss of cell viability, mitochondrial preparations are not studied *in vivo*. In  
325 contrast to isolated mitochondria and tissue homogenate preparations, mitochondria in  
326 permeabilized tissues and cells are *in situ* relative to the plasma membrane. The plasma  
327 membrane separates the intracellular compartment including the cytosol, nucleus, and  
328 organelles from the environment of the cell. The plasma membrane consists of a lipid bilayer,  
329 embedded proteins, and attached organic molecules that collectively control the selective  
330 permeability of ions, organic molecules, and particles across the cell boundary. The intact  
331 plasma membrane prevents the passage of many water-soluble mitochondrial substrates and  
332 inorganic ions—such as succinate, adenosine diphosphate (ADP) and inorganic phosphate (P<sub>i</sub>),

333 that must be controlled at kinetically-saturating concentrations for the analysis of respiratory  
334 capacities; this limits the scope of investigations into mitochondrial respiratory function in  
335 intact cells.

336 The cholesterol content of the plasma membrane is high compared to mitochondrial  
337 membranes. Therefore, mild detergents—such as digitonin and saponin—can be applied to  
338 selectively permeabilize the plasma membrane by interaction with cholesterol and allow free  
339 exchange of organic molecules and inorganic ions between the cytosol and the immediate cell  
340 environment, while maintaining the integrity and localization of organelles, cytoskeleton, and  
341 the nucleus. Application of optimum concentrations of permeabilization agents (mild detergents  
342 or toxins) leads to washout of cytosolic marker enzymes—such as lactate dehydrogenase—and  
343 results in the complete loss of cell viability, tested by nuclear staining using membrane-  
344 impermeable dyes, while mitochondrial function remains intact. Respiration of isolated  
345 mitochondria remains unaltered after the addition of low concentrations of digitonin or saponin.  
346 In addition to mechanical permeabilization during homogenization of tissue, permeabilization  
347 agents may be applied to ensure permeabilization of all cells. Suspensions of cells  
348 permeabilized in the respiration chamber and crude tissue homogenates contain all components  
349 of the cell at highly dilute concentrations. All mitochondria are retained in chemically-  
350 permeabilized mitochondrial preparations and crude tissue homogenates. In the preparation of  
351 isolated mitochondria, the cells or tissues are homogenized, and the mitochondria are separated  
352 from other cell fractions and purified by differential centrifugation, entailing the loss of a  
353 fraction of the total mitochondrial content. Typical mitochondrial recovery ranges from 30% to  
354 80%. Maximization of the purity of isolated mitochondria may compromise not only the  
355 mitochondrial yield but also the structural and functional integrity. Therefore, protocols to  
356 isolate mitochondria need to be optimized according to each study. The term mitochondrial  
357 preparation does not include further fractionation of mitochondrial components, neither  
358 submitochondrial particles.

359

### 360 2.1. Respiratory control and coupling

361

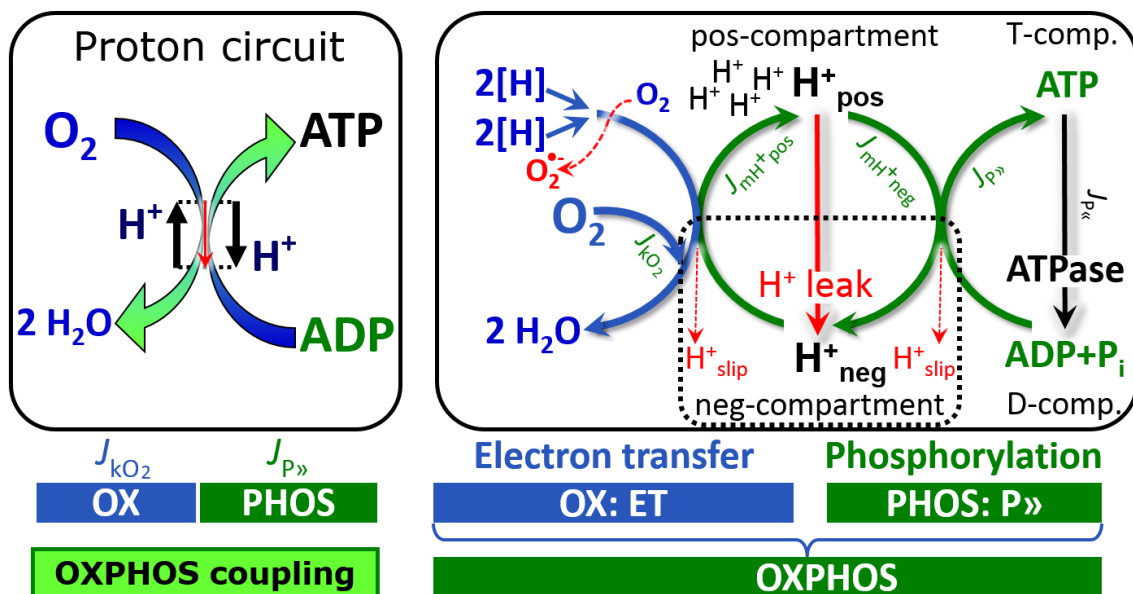
362 Respiratory coupling control states are established in studies of mitochondrial  
363 preparations to obtain reference values for various output variables. Physiological conditions *in*  
364 *vivo* deviate from these experimentally obtained states. Since kinetically-saturating  
365 concentrations, *e.g.*, of ADP or oxygen ( $O_2$ ; dioxygen), may not apply to physiological  
366 intracellular conditions, relevant information is obtained in studies of kinetic responses to  
367 variations in [ADP] or  $[O_2]$  in the range between kinetically-saturating concentrations and  
368 anoxia (Gnaiger 2001).

369 **The steady-state:** Mitochondria represent a thermodynamically open system in non-  
370 equilibrium states of biochemical energy transformation. State variables (protonmotive force;  
371 redox states) and metabolic *rates* (fluxes) are measured in defined mitochondrial respiratory  
372 *states*. Steady-states can be obtained only in open systems, in which changes by *internal*  
373 transformations, *e.g.*,  $O_2$  consumption, are instantaneously compensated for by *external* fluxes,  
374 *e.g.*,  $O_2$  supply, preventing a change of  $O_2$  concentration in the system (Gnaiger 1993b).  
375 Mitochondrial respiratory states monitored in closed systems satisfy the criteria of pseudo-  
376 steady states for limited periods of time, when changes in the system (concentrations of  $O_2$ , fuel  
377 substrates, ADP,  $P_i$ ,  $H^+$ ) do not exert significant effects on metabolic fluxes (respiration,  
378 phosphorylation). Such pseudo-steady states require respiratory media with sufficient buffering  
379 capacity and substrates maintained at kinetically-saturating concentrations, and thus depend on  
380 the kinetics of the processes under investigation.

381 **Specification of biochemical dose:** Substrates, uncouplers, inhibitors, and other  
382 biochemical reagents are titrated to dissect mitochondrial function. Nominal concentrations of  
383 these substances are usually reported as initial amount of substance concentration  $[\text{mol}\cdot\text{L}^{-1}]$  in



384 the incubation medium. When aiming at the measurement of kinetically saturated processes—  
 385 such as OXPHOS-capacities, the concentrations for substrates can be chosen according to the  
 386 apparent equilibrium constant,  $K_m'$ . In the case of hyperbolic kinetics, only 80% of maximum  
 387 respiratory capacity is obtained at a substrate concentration of four times the  $K_m'$ , whereas  
 388 substrate concentrations of 5, 9, 19 and 49 times the  $K_m'$  are theoretically required for reaching  
 389 83%, 90%, 95% or 98% of the maximal rate (Gnaiger 2001). Other reagents are chosen to  
 390 inhibit or alter some processes. The amount of these chemicals in an experimental incubation  
 391 is selected to maximize effect, avoiding unacceptable off-target consequences that would  
 392 adversely affect the data being sought. Specifying the amount of substance in an incubation as  
 393 nominal concentration in the aqueous incubation medium can be ambiguous (Doskey *et al.*  
 394 2015), particularly for lipophilic substances (oligomycin; uncouplers, permeabilization agents)  
 395 or cations (TPP<sup>+</sup>; fluorescent dyes such as safranin, TMRM), which accumulate in biological  
 396 membranes or in the mitochondrial matrix. For example, a dose of digitonin of 8 fmol·cell<sup>-1</sup> (10  
 397 pg·cell<sup>-1</sup>; 10 μg·10<sup>-6</sup> cells) is optimal for permeabilization of endothelial cells, and the  
 398 concentration in the incubation medium has to be adjusted according to the cell density applied  
 399 (Doerrier *et al.* 2018). Generally, dose/exposure can be specified per unit of biological sample,  
 400 *i.e.*, (nominal moles of xenobiotic)/(number of cells) [mol·cell<sup>-1</sup>] or, as appropriate, per mass of  
 401 biological sample [mol·kg<sup>-1</sup>]. This approach to specification of dose/exposure provides a  
 402 scalable parameter that can be used to design experiments, help interpret a wide variety of  
 403 experimental results, and provide absolute information that allows researchers worldwide to  
 404 make the most use of published data (Doskey *et al.* 2015).  
 405



406  
 407 **Fig. 2. The proton circuit and coupling in oxidative phosphorylation (OXPHOS).**  $2[H]$   
 408 indicates the reduced hydrogen equivalents of fuel substrates of the catabolic reaction  $k$  with  
 409 oxygen.  $O_2$  flux,  $J_{kO_2}$ , through the catabolic ET-pathway, is coupled to flux through the  
 410 phosphorylation-pathway of  $ADP$  to  $ATP$ ,  $J_{P\gg}$ . The proton pumps of the ET-pathway drive  
 411 proton flux into the positive (pos) compartment,  $J_{mH^+pos}$ , generating the output protonmotive  
 412 force (motive, subscript  $m$ ). F-ATPase is coupled to inward proton current into the negative  
 413 (neg) compartment,  $J_{mH^+neg}$ , to phosphorylate  $ADP+P_i$  to  $ATP$ . The system defined by the  
 414 boundaries (full black line) is not a black box, but is analysed as a compartmental system. The  
 415 negative compartment (neg-compartment, enclosed by the dotted line) is the matrix space,  
 416 separated by the mtIM from the positive compartment (pos-compartment).  $ADP+P_i$  and  $ATP$   
 417 are the substrate- and product-compartments (scalar  $ADP$  and  $ATP$  compartments, D-comp.  
 418 and T-comp.), respectively. At steady-state proton turnover,  $J_{\infty H^+}$ , and  $ATP$  turnover,  $J_{\infty P}$ ,

419 maintain concentrations constant, when  $J_{mH^{+\infty}} = J_{mH^{+pos}} = J_{mH^{+neg}}$ , and  $J_{P_{\infty}} = J_{P_{\gg}} = J_{P_{\ll}}$ . Modified  
 420 from Gnaiger (2014).

421

422 **Phosphorylation, P $\gg$ , and P $\gg$ /O $_2$  ratio:** *Phosphorylation* in the context of OXPHOS is  
 423 defined as phosphorylation of ADP by P $_i$  to ATP. On the other hand, the term phosphorylation  
 424 is used generally in many contexts, *e.g.*, protein phosphorylation. This justifies consideration  
 425 of a symbol more discriminating and specific than P as used in the P/O ratio (phosphate to  
 426 atomic oxygen ratio), where P indicates phosphorylation of ADP to ATP or GDP to GTP. We  
 427 propose the symbol P $\gg$  for the endergonic (uphill) direction of phosphorylation ADP $\rightarrow$ ATP,  
 428 and likewise the symbol P $\ll$  for the corresponding exergonic (downhill) hydrolysis ATP $\rightarrow$ ADP  
 429 (**Fig. 2**). P $\gg$  refers mainly to electrontransfer phosphorylation but may also involve substrate-  
 430 level phosphorylation as part of the tricarboxylic acid (TCA) cycle (succinyl-CoA ligase) and  
 431 phosphorylation of ADP catalyzed by phosphoenolpyruvate carboxykinase.  
 432 Transphosphorylation is performed by adenylate kinase, creatine kinase, hexokinase and  
 433 nucleoside diphosphate kinase. In isolated mammalian mitochondria, ATP production  
 434 catalyzed by adenylate kinase (2 ADP  $\leftrightarrow$  ATP + AMP) proceeds without fuel substrates in the  
 435 presence of ADP (Komlódi and Tretter 2017). Kinase cycles are involved in intracellular energy  
 436 transfer and signal transduction for regulation of energy flux.

437 The P $\gg$ /O $_2$  ratio (P $\gg$ /4 e $^-$ ) is two times the ‘P/O’ ratio (P $\gg$ /2 e $^-$ ) of classical bioenergetics.  
 438 P $\gg$ /O $_2$  is a generalized symbol, independent phosphorylation assessment by determination of P $_i$   
 439 consumption (P $_i$ /O $_2$  flux ratio), ADP depletion (ADP/O $_2$  flux ratio), or ATP production  
 440 (ATP/O $_2$  flux ratio). The mechanistic P $\gg$ /O $_2$  ratio—or P $\gg$ /O $_2$  stoichiometry—is calculated from  
 441 the proton-to-O $_2$  and proton-to-phosphorylation coupling stoichiometries (**Fig. 1A**),  
 442

$$443 \quad P_{\gg}/O_2 = \frac{H_{pos}^+/O_2}{H_{neg}^+/P_{\gg}} \quad (1)$$

444

445 The H $^+_{pos}$ /O $_2$  *coupling stoichiometry* (referring to the full 4 electron reduction of O $_2$ ) depends  
 446 on the ET-pathway control state which defines the relative involvement of the three coupling  
 447 sites (CI, CIII and CIV) in the catabolic pathway of electrons to O $_2$ . This varies with: (1) a  
 448 bypass of CI by single or multiple electron input into the Q-junction; and (2) a bypass of CIV  
 449 by involvement of AOX. H $^+_{pos}$ /O $_2$  is 12 in the ET-pathways involving CIII and CIV as proton  
 450 pumps, increasing to 20 for the NADH-pathway (**Fig. 1A**), but a general consensus on H $^+_{pos}$ /O $_2$   
 451 stoichiometries remains to be reached (Hinkle 2005; Wikström and Hummer 2012; Sazanov  
 452 2015). The H $^+_{neg}$ /P $\gg$  coupling stoichiometry (3.7; **Fig. 1A**) is the sum of 2.7 H $^+_{neg}$  required by  
 453 the F-ATPase of vertebrate and most invertebrate species (Watt *et al.* 2010) and the proton  
 454 balance in the translocation of ADP, ATP and P $_i$  (**Fig. 1B**). Taken together, the mechanistic  
 455 P $\gg$ /O $_2$  ratio is calculated at 5.4 and 3.3 for NADH- and succinate-linked respiration, respectively  
 456 (Eq. 1). The corresponding classical P $\gg$ /O ratios (referring to the 2 electron reduction of 0.5 O $_2$ )  
 457 are 2.7 and 1.6 (Watt *et al.* 2010), in agreement with the measured P $\gg$ /O ratio for succinate of  
 458  $1.58 \pm 0.02$  (Gnaiger *et al.* 2000).

459 The effective P $\gg$ /O $_2$  flux ratio ( $Y_{P_{\gg}/O_2} = J_{P_{\gg}}/J_{kO_2}$ ) is diminished relative to the mechanistic  
 460 P $\gg$ /O $_2$  ratio by intrinsic and extrinsic uncoupling and dyscoupling (**Fig. 3**). Such generalized  
 461 uncoupling is different from switching to mitochondrial pathways that involve fewer than three  
 462 proton pumps (‘coupling sites’: Complexes CI, CIII and CIV), bypassing CI through multiple  
 463 electron entries into the Q-junction, or CIII and CIV through AOX (**Fig. 1**). Reprogramming of  
 464 mitochondrial pathways may be considered as a switch of gears (changing the stoichiometry)  
 465 rather than uncoupling (loosening the stoichiometry). In addition,  $Y_{P_{\gg}/O_2}$  depends on several  
 466 experimental conditions of flux control, increasing as a hyperbolic function of [ADP] to a  
 467 maximum value (Gnaiger 2001).

468       **Control and regulation:** The terms metabolic *control* and *regulation* are frequently used  
 469 synonymously, but are distinguished in metabolic control analysis: ‘We could understand the  
 470 regulation as the mechanism that occurs when a system maintains some variable constant over  
 471 time, in spite of fluctuations in external conditions (homeostasis of the internal state). On the  
 472 other hand, metabolic control is the power to change the state of the metabolism in response to  
 473 an external signal’ (Fell 1997). Respiratory control may be induced by experimental control  
 474 signals that *exert* an influence on: (1) ATP demand and ADP phosphorylation-rate; (2) fuel  
 475 substrate composition, pathway competition; (3) available amounts of substrates and O<sub>2</sub>, *e.g.*,  
 476 starvation and hypoxia; (4) the protonmotive force, redox states, flux–force relationships,  
 477 coupling and efficiency; (5) Ca<sup>2+</sup> and other ions including H<sup>+</sup>; (6) inhibitors, *e.g.*, nitric oxide  
 478 or intermediary metabolites such as oxaloacetate; (7) signalling pathways and regulatory  
 479 proteins, *e.g.*, insulin resistance, transcription factor hypoxia inducible factor 1. *Mechanisms* of  
 480 respiratory control and regulation include adjustments of: (1) enzyme activities by allosteric  
 481 mechanisms and phosphorylation; (2) enzyme content, concentrations of cofactors and  
 482 conserved moieties—such as adenylates, nicotinamide adenine dinucleotide [NAD<sup>+</sup>/NADH],  
 483 coenzyme Q, cytochrome *c*; (3) metabolic channeling by supercomplexes; and (4)  
 484 mitochondrial density (enzyme concentrations and membrane area) and morphology (cristae  
 485 folding, fission and fusion). Mitochondria are targeted directly by hormones, thereby affecting  
 486 their energy metabolism (Lee *et al.* 2013; Gerö and Szabo 2016; Price and Dai 2016; Moreno  
 487 *et al.* 2017). Evolutionary or acquired differences in the genetic and epigenetic basis of  
 488 mitochondrial function (or dysfunction) between subjects and gene therapy; age; gender,  
 489 biological sex, and hormone concentrations; life style including exercise and nutrition; and  
 490 environmental issues including thermal, atmospheric, toxicological and pharmacological  
 491 factors, exert an influence on all control mechanisms listed above. For reviews, see Brown  
 492 1992; Gnaiger 1993a, 2009; 2014; Paradies *et al.* 2014; Morrow *et al.* 2017.

493       **Respiratory control and response:** Lack of control by a metabolic pathway, *e.g.*,  
 494 phosphorylation-pathway, means that there will be no response to a variable activating it, *e.g.*,  
 495 [ADP]. The reverse, however, is not true as the absence of a response to [ADP] does not exclude  
 496 the phosphorylation-pathway from having some degree of control. The degree of control of a  
 497 component of the OXPHOS-pathway on an output variable—such as O<sub>2</sub> flux, will in general  
 498 be different from the degree of control on other outputs—such as phosphorylation-flux or  
 499 proton leak flux. Therefore, it is necessary to be specific as to which input and output are under  
 500 consideration (Fell 1997).

501       **Respiratory coupling control and ET-pathway control:** Respiratory control refers to  
 502 the ability of mitochondria to adjust O<sub>2</sub> flux in response to external control signals by engaging  
 503 various mechanisms of control and regulation. Respiratory control is monitored in a  
 504 mitochondrial preparation under conditions defined as respiratory states. When  
 505 phosphorylation of ADP to ATP is stimulated or depressed, an increase or decrease is observed  
 506 in electron flux linked to O<sub>2</sub> flux in respiratory coupling states of intact mitochondria  
 507 (‘controlled states’ in the classical terminology of bioenergetics). Alternatively, coupling of  
 508 electron transfer with phosphorylation is disengaged by disruption of the integrity of the mtIM  
 509 or by uncouplers, functioning like a clutch in a mechanical system. The corresponding coupling  
 510 control state is characterized by high levels of O<sub>2</sub> consumption without control by P»  
 511 (‘uncontrolled state’).

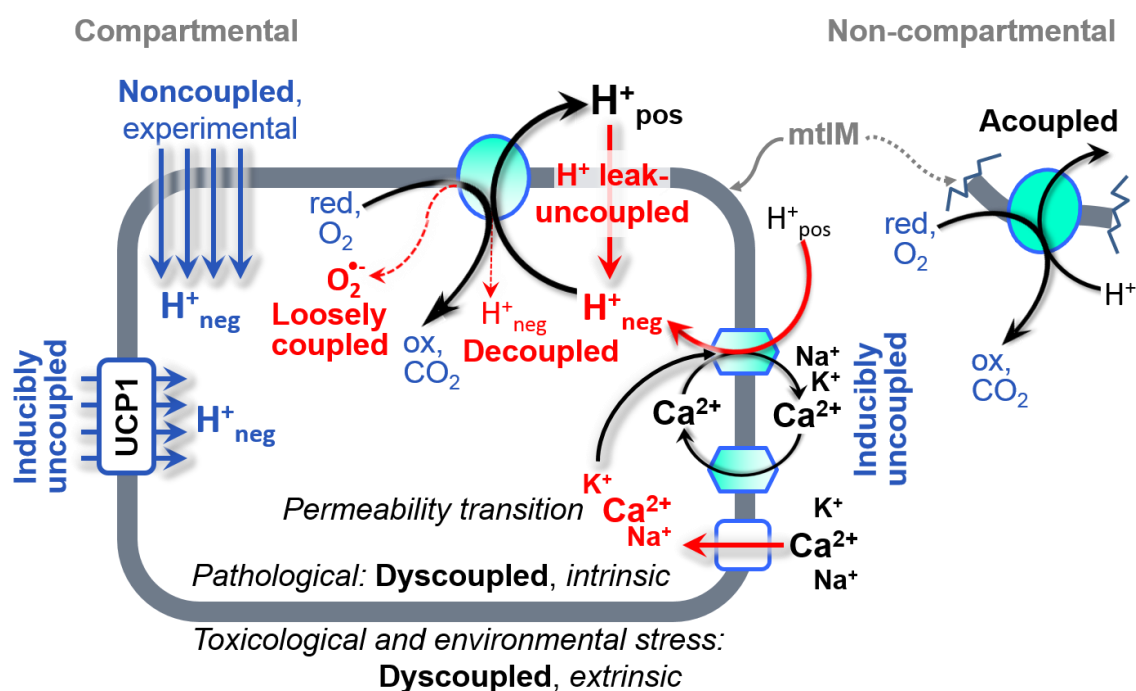
512       ET-pathway control states are obtained in mitochondrial preparations by depletion of  
 513 endogenous substrates and addition to the mitochondrial respiration medium of fuel substrates  
 514 (CHNO; 2[H] in **Fig. 2**) and specific inhibitors, activating selected mitochondrial catabolic  
 515 pathways, *k* (**Fig. 1**). Coupling control states and pathway control states are complementary,  
 516 since mitochondrial preparations depend on an exogenous supply of pathway-specific fuel  
 517 substrates and oxygen (Gnaiger 2014).

518 **Coupling:** In mitochondrial electron transfer (**Fig. 1**), vectorial transmembrane proton  
 519 flux is coupled through the proton pumps CI, CIII and CIV to the catabolic flux of scalar  
 520 reactions, collectively measured as O<sub>2</sub> flux (**Fig. 2**). Thus mitochondria are elements of energy  
 521 transformation. Energy cannot be lost or produced in any internal process (First Law of  
 522 thermodynamics). Open and closed systems can gain or loose energy only by external fluxes—  
 523 by exchange with the environment. Energy is a conserved quantity. Therefore, energy can  
 524 neither be produced by mitochondria, nor is there any internal process without energy  
 525 conservation. Exergy is defined as the ‘free energy’ with the potential to perform work.  
 526 *Coupling* is the mechanistic linkage of an exergonic process (spontaneous, negative exergy  
 527 change) with an endergonic process (positive exergy change) in energy transformations which  
 528 conserve part of the exergy that would be irreversible lost or dissipated in an uncoupled process.

529 **Uncoupling:** Uncoupling of mitochondrial respiration is a general term comprising  
 530 diverse mechanisms. Differences of terms—uncoupled vs. noncoupled—are easily overlooked,  
 531 although they relate to different mechanisms of uncoupling (**Fig. 3**).

- 532 1. Proton leak across the mtIM from the pos- to the neg-compartment (**Fig. 2**);
- 533 2. Cycling of other cations, strongly stimulated by permeability transition;
- 534 3. Proton slip in the proton pumps when protons are effectively not pumped (CI, CIII and  
 535 CIV) or are not driving phosphorylation (F-ATPase);
- 536 4. Loss of compartmental integrity when electron transfer is acoupled;
- 537 5. Electron leak in the loosely coupled univalent reduction of O<sub>2</sub> to superoxide (O<sub>2</sub><sup>•-</sup>;  
 538 superoxide anion radical).

539



540

541 **Fig 3. Mechanisms of respiratory uncoupling.** An intact mitochondrial inner membrane,  
 542 mtIM, is required for vectorial, compartmental coupling. ‘Acoupled’ respiration is the  
 543 consequence of structural disruption with catalytic activity of non-compartmental  
 544 mitochondrial fragments. Inducibly uncoupled (activation of UCP1) and experimentally  
 545 noncoupled respiration (titration of protonophores) stimulate respiration to maximum O<sub>2</sub> flux.  
 546 H<sup>+</sup> leak-uncoupled, decoupled, and loosely coupled respiration are components of intrinsic  
 547 uncoupling. Pathological dysfunction may affect all types of uncoupling, including  
 548 permeability transition, causing intrinsically dyscoupled respiration. Similarly, toxicological  
 549 and environmental stress factors can cause extrinsically dyscoupled respiration.

550



## 551 2.2. Coupling states and respiratory rates

552

553 **Respiratory capacities in coupling control states:** To extend the classical nomenclature  
 554 on mitochondrial coupling states (Section 2.3) by a concept-driven terminology that  
 555 incorporates explicitly information on the nature of respiratory states, the terminology must be  
 556 general and not restricted to any particular experimental protocol or mitochondrial preparation  
 557 (Gnaiger 2009). We focus primarily on the conceptual ‘why’, along with clarification of the  
 558 experimental ‘how’. Respiratory capacities delineate, comparable to channel capacity in  
 559 information theory (Schneider 2006), the upper bound of the rate of respiration measured in  
 560 defined coupling control states and electron transfer-pathway (ET-pathway) states (**Fig. 4**).

561

562 **Fig. 4. Four-compartment**563 **model of oxidative**564 **phosphorylation.**

565 Respiratory

566 states (ET, OXPHOS, LEAK;

567 **Table 1**) and corresponding rates568 ( $E$ ,  $P$ ,  $L$ ) are connected by the569 protonmotive force,  $\Delta p$ . ET-570 capacity,  $E$ , is partitioned into (1)571 dissipative LEAK-respiration,  $L$ ,

572 when the Gibbs energy change of

573 catabolic  $O_2$  flux is irreversibly574 lost, (2) net OXPHOS-capacity,  $P-L$ ,

575 with partial conservation of the capacity to perform work,

576 and (3) the excess capacity,  $E-P$ . Modified from Gnaiger (2014).

577

578

579

580

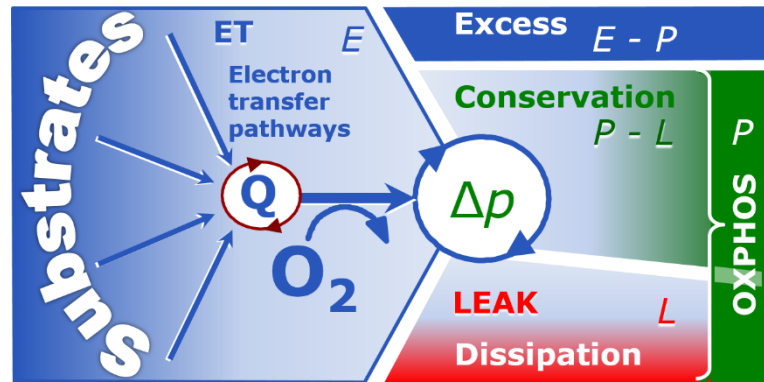


**Table 1. Coupling states and residual oxygen consumption in mitochondrial preparations in relation to respiration- and phosphorylation-flux,  $J_{kO_2}$  and  $J_{P_{\gg}}$ , and protonmotive force,  $\Delta p$ .** Coupling states are established at kinetically-saturating concentrations of fuel substrates and  $O_2$ .

State	$J_{kO_2}$	$J_{P_{\gg}}$	$\Delta p$	Inducing factors	Limiting factors
LEAK	$L$ ; low, cation leak-dependent respiration	0	max.	proton leak, slip, and cation cycling	$J_{P_{\gg}} = 0$ : (1) without ADP, $L_N$ ; (2) max. ATP/ADP ratio, $L_T$ ; or (3) inhibition of the phosphorylation-pathway, $L_{Omy}$
OXPHOS	$P$ ; high, ADP-stimulated respiration	max.	high	kinetically-saturating [ADP] and $[P_i]$	$J_{P_{\gg}}$ by phosphorylation-pathway; or $J_{kO_2}$ by ET-capacity
ET	$E$ ; max., noncoupled respiration	0	low	optimal external uncoupler concentration for max. $J_{O_2,E}$	$J_{kO_2}$ by ET-capacity
ROX	$R_{ox}$ ; min., residual $O_2$ consumption	0	0	$J_{O_2,Rox}$ in non-ET-pathway oxidation reactions	full inhibition of ET-pathway; or absence of fuel substrates

581



582 To provide a diagnostic reference for respiratory capacities of core energy metabolism,  
 583 the capacity of *oxidative phosphorylation*, OXPHOS, is measured at kinetically-saturating  
 584 concentrations of ADP and  $P_i$ . The *oxidative* ET-capacity reveals the limitation of OXPHOS-  
 585 capacity mediated by the *phosphorylation*-pathway. The ET- and phosphorylation-pathways  
 586 comprise coupled segments of the OXPHOS-system. ET-capacity is measured as noncoupled  
 587 respiration by application of *external uncouplers*. The contribution of *intrinsically uncoupled*  
 588  $O_2$  consumption is studied in the absence of ADP—by not stimulating phosphorylation, or by  
 589 inhibition of the phosphorylation-pathway. The corresponding states are collectively classified  
 590 as LEAK-states, when  $O_2$  consumption compensates mainly for ion leaks, including the proton  
 591 leak. Defined coupling states are induced by: (1) adding cation chelators such as EGTA, binding  
 592 free  $Ca^{2+}$  and thus limiting cation cycling; (2) adding ADP and  $P_i$ ; (3) inhibiting the  
 593 phosphorylation-pathway; and (4) uncoupler titrations, while maintaining a defined ET-  
 594 pathway state with constant fuel substrates and inhibitors of specific branches of the ET-  
 595 pathway (**Fig. 1**).

596 The three coupling states, ET, LEAK and OXPHOS, are shown schematically with the  
 597 corresponding respiratory rates, abbreviated as  $E$ ,  $L$  and  $P$ , respectively (**Fig. 4**). We distinguish  
 598 metabolic *pathways* from metabolic *states* and the corresponding metabolic *rates*; for example:  
 599 ET-pathways (**Fig. 4**), ET-state (**Fig. 5C**), and ET-capacity,  $E$ , respectively (**Table 1**). The  
 600 protonmotive force is *high* in the OXPHOS-state when it drives phosphorylation, *maximum* in  
 601 the LEAK-state of coupled mitochondria, driven by LEAK-respiration at a minimum back flux  
 602 of cations to the matrix side, and *very low* in the ET-state when uncouplers short-circuit the  
 603 proton cycle (**Table 1**).

604  $E$  may exceed or be equal to  $P$ .  $E > P$  is observed in many types of mitochondria, varying  
 605 between species, tissues and cell types (Gnaiger 2009).  $E - P$  is the excess ET-capacity pushing  
 606 the phosphorylation-flux (**Fig. 1B**) to the limit of its *capacity of utilizing* the protonmotive force.  
 607 In addition, the magnitude of  $E - P$  depends on the tightness of respiratory coupling or degree of  
 608 uncoupling, since an increase of  $L$  causes  $P$  to increase towards the limit of  $E$ . The *excess*  $E - P$   
 609 capacity,  $E - P$ , therefore, provides a sensitive diagnostic indicator of specific injuries of the  
 610 phosphorylation-pathway, under conditions when  $E$  remains constant but  $P$  declines relative to  
 611 controls (**Fig. 4**). Substrate cocktails supporting simultaneous convergent electron transfer to  
 612 the Q-junction for reconstitution of TCA cycle function establish pathway control states with  
 613 high ET-capacity, and consequently increase the sensitivity of the  $E - P$  assay.

614  $E$  cannot theoretically be lower than  $P$ .  $E < P$  must be discounted as an artefact, which  
 615 may be caused experimentally by: (1) loss of oxidative capacity during the time course of the  
 616 respirometric assay, since  $E$  is measured subsequently to  $P$ ; (2) using insufficient uncoupler  
 617 concentrations; (3) using high uncoupler concentrations which inhibit ET (Gnaiger 2008); (4)  
 618 high oligomycin concentrations applied for measurement of  $L$  before titrations of uncoupler,  
 619 when oligomycin exerts an inhibitory effect on  $E$ . On the other hand, the excess ET-capacity is  
 620 overestimated if non-saturating  $[ADP]$  or  $[P_i]$  are used. See State 3 in the next section.

621 The net OXPHOS-capacity is calculated by subtracting  $L$  from  $P$  (**Fig. 4**). Then the net  
 622  $P \gg O_2$  equals  $P \gg (P - L)$ , wherein the dissipative LEAK component in the OXPHOS-state may  
 623 be overestimated. This can be avoided by measuring LEAK-respiration in a state when the  
 624 protonmotive force is adjusted to its slightly lower value in the OXPHOS-state—by titration of  
 625 an ET inhibitor (Divakaruni and Brand 2011). Any turnover-dependent components of proton  
 626 leak and slip, however, are underestimated under these conditions (Garlid *et al.* 1993). In  
 627 general, it is inappropriate to use the term *ATP production* or *ATP turnover* for the difference  
 628 of  $O_2$  flux measured in states  $P$  and  $L$ . The difference  $P - L$  is the upper limit of the part of  
 629 OXPHOS-capacity that is freely available for ATP production (corrected for LEAK-  
 630 respiration) and is fully coupled to phosphorylation with a maximum mechanistic stoichiometry  
 631 (**Fig. 4**).

632 **LEAK-state (Fig. 5A):**  
 633 The LEAK-state is defined as a  
 634 state of mitochondrial respiration  
 635 when  $O_2$  flux mainly  
 636 compensates for ion leaks in the  
 637 absence of ATP synthesis, at  
 638 kinetically-saturating  
 639 concentrations of  $O_2$  and  
 640 respiratory fuel substrates.  
 641 LEAK-respiration is measured to  
 642 obtain an estimate of *intrinsic*  
 643 *uncoupling* without addition of  
 644 an experimental uncoupler: (1) in  
 645 the absence of adenylates; (2)  
 646 after depletion of ADP at a  
 647 maximum ATP/ADP ratio; or (3)  
 648 after inhibition of the  
 649 phosphorylation-pathway by  
 650 inhibitors of F-ATPase—such as  
 651 oligomycin, or of adenine  
 652 nucleotide translocase—such as  
 653 carboxyatractyloside.  
 654 Adjustment of the nominal  
 655 concentration of these inhibitors  
 656 to the density of biological  
 657 sample applied can minimize or  
 658 avoid inhibitory side-effects  
 659 exerted on ET-capacity or even  
 660 some dyscoupling.

661 **Proton leak and**  
 662 **uncoupled respiration:** Proton  
 663 leak is a leak current of protons.  
 664 The intrinsic proton leak is the  
 665 *uncoupled* process in which  
 666 protons diffuse across the mtIM  
 667 in the dissipative direction of the  
 668 downhill protonmotive force  
 669 without coupling to  
 670 phosphorylation (Fig. 5A). The  
 671 proton leak flux depends non-  
 672 linearly on the protonmotive  
 673 force (Garlid *et al.* 1989;  
 674 Divakaruni and Brand 2011), it is a property of the mtIM and may be enhanced due to possible  
 675 contaminations by free fatty acids. Inducible uncoupling mediated by uncoupling protein 1  
 676 (UCP1) is physiologically controlled, *e.g.*, in brown adipose tissue. UCP1 is a member of the  
 677 mitochondrial carrier family which is involved in the translocation of protons across the mtIM  
 678 (Klingenberg 2017). Consequently, the short-circuit diminishes the protonmotive force and  
 679 stimulates electron transfer to  $O_2$  and heat dissipation without phosphorylation of ADP.

680 **Cation cycling:** There can be other cation contributors to leak current including calcium  
 681 and probably magnesium. Calcium current is balanced by mitochondrial  $Na^+/Ca^{2+}$  exchange,

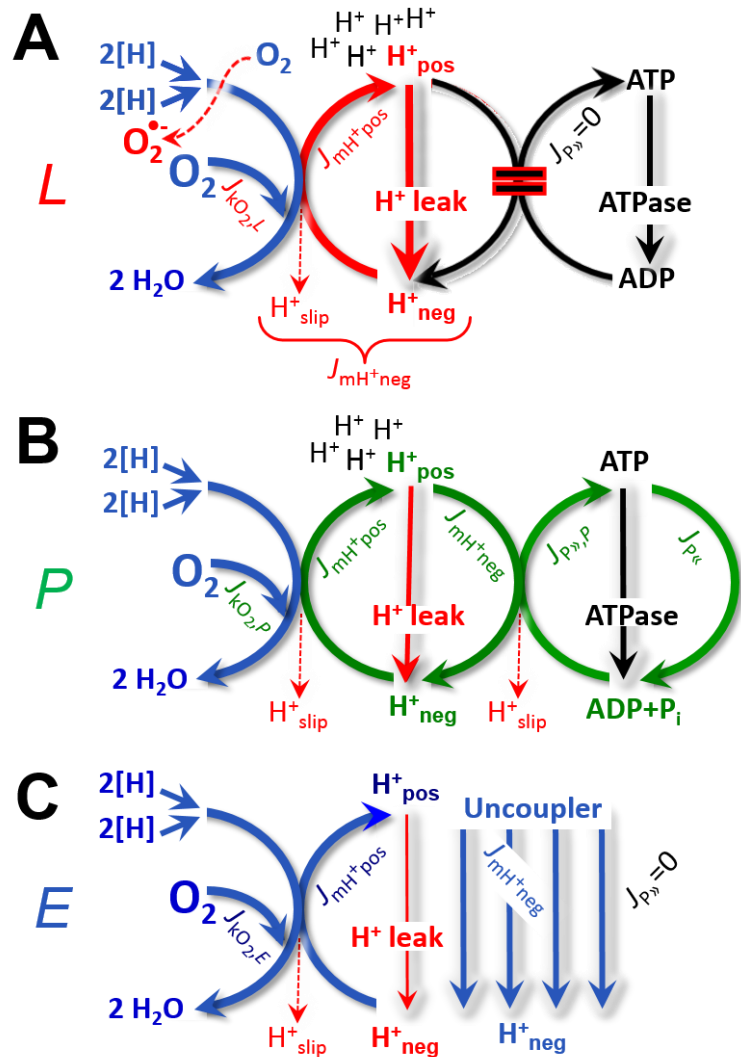


**Fig. 5. Respiratory coupling states. A: LEAK-state and rate, L:** Phosphorylation is arrested,  $J_{P_{\gg}} = 0$ , and catabolic  $O_2$  flux,  $J_{kO_2,L}$ , is controlled mainly by the proton leak,  $J_{mH^{+neg},L}$ , at maximum protonmotive force (Fig. 3). **B: OXPHOS-state and rate, P:** Phosphorylation,  $J_{P_{\gg}}$ , is stimulated by kinetically-saturating [ADP] and  $[P_i]$ , and is supported by a high protonmotive force.  $O_2$  flux,  $J_{kO_2,P}$ , is well-coupled at a  $P_{\gg}/O_2$  ratio of  $J_{P_{\gg},P}/J_{kO_2,P}$ . **C: ET-state and rate, E:** Noncoupled respiration,  $J_{kO_2,E}$ , is maximum at optimum exogenous uncoupler concentration and phosphorylation is zero,  $J_{P_{\gg}} = 0$ . See also Fig. 2.

682 which is balanced by  $\text{Na}^+/\text{H}^+$  or  $\text{K}^+/\text{H}^+$  exchanges. This is another effective uncoupling  
683 mechanism different from proton leak.

684

685 **Table 2. Terms on respiratory coupling and uncoupling.**

Term	$J_{\text{kO}_2}$	$\text{P}\gg/\text{O}_2$	Note	
acoupled		0	electron transfer in mitochondrial fragments without vectorial proton translocation ( <b>Fig. 3</b> )	
intrinsic, no protonophore added	uncoupled	$L$	0	non-phosphorylating LEAK-respiration ( <b>Fig. 5A</b> )
	proton leak-uncoupled		0	component of $L$ , $\text{H}^+$ diffusion across the mtIM ( <b>Fig. 3</b> )
	decoupled		0	component of $L$ , proton slip ( <b>Fig. 3</b> )
	loosely coupled		0	component of $L$ , lower coupling due to superoxide formation and bypass of proton pumps ( <b>Fig. 3</b> )
	dyscoupled		0	pathologically, toxicologically, environmentally increased uncoupling, mitochondrial dysfunction
	inducibly uncoupled		0	by UCP1 or cation ( <i>e.g.</i> , $\text{Ca}^{2+}$ ) cycling ( <b>Fig. 3</b> )
noncoupled	$E$	0	non-phosphorylating respiration stimulated to maximum flux at optimum exogenous uncoupler concentration ( <b>Fig. 5C</b> )	
well-coupled	$P$	high	phosphorylating respiration with an intrinsic LEAK component ( <b>Fig. 5B</b> )	
fully coupled	$P - L$	max.	OXPHOS-capacity corrected for LEAK-respiration ( <b>Fig. 4</b> )	

686

687

688

689

690

691

692

693

694

695

**Proton slip and decoupled respiration:** Proton slip is the *decoupled* process in which protons are only partially translocated by a proton pump of the ET-pathways and slip back to the original compartment. The proton leak is the dominant contributor to the overall leak current in mammalian mitochondria incubated under physiological conditions at 37 °C, whereas proton slip is increased at lower experimental temperature (Canton *et al.* 1995). Proton slip can also happen in association with the F-ATPase, in which the proton slips downhill across the pump to the matrix without contributing to ATP synthesis. In each case, proton slip is a property of the proton pump and increases with the pump turnover rate.

696

697

698

699

**Electron leak and loosely coupled respiration:** Superoxide production by the ETS leads to a bypass of proton pumps and correspondingly lower  $\text{P}\gg/\text{O}_2$  ratio. This depends on the actual site of electron leak and the scavenging of hydrogen peroxide by cytochrome *c*, whereby electrons may re-enter the ETS with proton translocation by CIV.

700

701

702

703

704

**Loss of compartmental integrity and acoupled respiration:** Electron transfer and catabolic  $\text{O}_2$  flux proceed without compartmental proton translocation in disrupted mitochondrial fragments. Such fragments form during mitochondrial isolation, and may not fully fuse to re-establish structurally intact mitochondria. Loss of mtIM integrity, therefore, is the cause of acoupled respiration, which is a nonvectorial dissipative process without control by the protonmotive force.

705

706

707

**Dyscoupled respiration:** Mitochondrial injuries may lead to *dyscoupling* as a pathological or toxicological cause of *uncoupled* respiration. Dyscoupling may involve any type of uncoupling mechanism, *e.g.*, opening the permeability transition pore. Dyscoupled

708 respiration is distinguished from the experimentally induced *noncoupled* respiration in the ET-  
709 state (**Fig. 3**).

710 **OXPHOS-state (Fig. 5B)**: The OXPHOS-state is defined as the respiratory state with  
711 kinetically-saturating concentrations of O<sub>2</sub>, respiratory and phosphorylation substrates, and  
712 absence of exogenous uncoupler, which provides an estimate of the maximal respiratory  
713 capacity in the OXPHOS-state for any given ET-pathway state. Respiratory capacities at  
714 kinetically-saturating substrate concentrations provide reference values or upper limits of  
715 performance, aiming at the generation of data sets for comparative purposes. Physiological  
716 activities and effects of substrate kinetics can be evaluated relative to the OXPHOS-capacity.

717 As discussed previously, 0.2 mM ADP does not fully saturate flux in isolated  
718 mitochondria (Gnaiger 2001; Puchowicz *et al.* 2004); greater ADP concentration is required,  
719 particularly in permeabilized muscle fibres and cardiomyocytes, to overcome limitations by  
720 intracellular diffusion and by the reduced conductance of the mtOM (Jepihhina *et al.* 2011,  
721 Illaste *et al.* 2012, Simson *et al.* 2016), either through interaction with tubulin (Rostovtseva *et al.*  
722 2008) or other intracellular structures (Birkedal *et al.* 2014). In permeabilized muscle fibre  
723 bundles of high respiratory capacity, the apparent  $K_m$  for ADP increases up to 0.5 mM (Saks *et al.*  
724 1998), consistent with experimental evidence that >90% saturation is reached only at >5  
725 mM ADP (Pesta and Gnaiger 2012). Similar ADP concentrations are also required for accurate  
726 determination of OXPHOS-capacity in human clinical cancer samples and permeabilized cells  
727 (Klepinin *et al.* 2016; Koit *et al.* 2017). Whereas 2.5 to 5 mM ADP is sufficient to obtain the  
728 actual OXPHOS-capacity in many types of permeabilized tissue and cell preparations,  
729 experimental validation is required in each specific case.

730 **Electron transfer-state (Fig. 5C)**: The ET-state is defined as the *noncoupled* state with  
731 kinetically-saturating concentrations of O<sub>2</sub>, respiratory substrate and optimum *exogenous*  
732 uncoupler concentration for maximum O<sub>2</sub> flux. O<sub>2</sub> flux determined in the ET-state yields an  
733 estimate of ET-capacity. Inhibition of respiration is observed at higher than optimum uncoupler  
734 concentrations. As a consequence of the nearly collapsed protonmotive force, the driving force  
735 is insufficient for phosphorylation, and  $J_{P_s} = 0$ .

736 **ROX state and Rox**: Besides the three fundamental coupling states of mitochondrial  
737 preparations, the state of residual O<sub>2</sub> consumption, ROX, is relevant to assess respiratory  
738 function. ROX is not a coupling state. The rate of residual oxygen consumption, *Rox*, is defined  
739 as O<sub>2</sub> consumption due to oxidative side reactions measured after inhibition of ET—with  
740 rotenone, malonic acid and antimycin A. Cyanide and azide inhibit CIV and several peroxidases  
741 involved in *Rox*. ROX represents a baseline that is used to correct respiration in defined  
742 coupling states. *Rox* is not necessarily equivalent to non-mitochondrial respiration, considering  
743 O<sub>2</sub>-consuming reactions in mitochondria not related to ET—such as O<sub>2</sub> consumption in  
744 reactions catalyzed by monoamine oxidases (type A and B), monooxygenases (cytochrome  
745 P450 monooxygenases), dioxygenase (sulfur dioxygenase and trimethyllysine dioxygenase),  
746 and several hydroxylases. Mitochondrial preparations, especially those obtained from liver, may  
747 be contaminated by peroxisomes. This fact makes the exact determination of mitochondrial O<sub>2</sub>  
748 consumption and mitochondria-associated generation of reactive oxygen species complicated  
749 (Schönfeld *et al.* 2009). The dependence of ROX-linked O<sub>2</sub> consumption needs to be studied  
750 in detail together with non-ET enzyme activities, availability of specific substrates, O<sub>2</sub>  
751 concentration, and electron leakage leading to the formation of reactive oxygen species.

### 752 2.3. Classical terminology for isolated mitochondria

754 'When a code is familiar enough, it ceases appearing like a code; one forgets that there  
755 is a decoding mechanism. The message is identical with its meaning' (Hofstadter 1979).

756  
757 Chance and Williams (1955; 1956) introduced five classical states of mitochondrial respiration  
758 and cytochrome redox states. **Table 3** shows a protocol with isolated mitochondria in a closed



759 respirometric chamber, defining a sequence of respiratory states. States and rates are not  
760 specifically distinguished in this nomenclature.

761  
762  
763  
764

**Table 3. Metabolic states of mitochondria (Chance and Williams, 1956; Table V).**

State	[O <sub>2</sub> ]	ADP level	Substrate level	Respiration rate	Rate-limiting substance
1	>0	low	low	slow	ADP
2	>0	high	~0	slow	Substrate
3	>0	high	high	fast	respiratory chain
4	>0	low	high	slow	ADP
5	0	high	high	0	Oxygen

765

766 **State 1** is obtained after addition of isolated mitochondria to air-saturated  
767 isoosmotic/isotonic respiration medium containing P<sub>i</sub>, but no fuel substrates and no adenylates,  
768 *i.e.*, AMP, ADP, ATP.

769 **State 2** is induced by addition of a ‘high’ concentration of ADP (typically 100 to 300  
770 μM), which stimulates respiration transiently on the basis of endogenous fuel substrates and  
771 phosphorylates only a small portion of the added ADP. State 2 is then obtained at a low  
772 respiratory activity limited by exhausted endogenous fuel substrate availability (**Table 3**). If  
773 addition of specific inhibitors of respiratory complexes—such as rotenone—does not cause a  
774 further decline of O<sub>2</sub> flux, State 2 is equivalent to the ROX state (See below.). If inhibition is  
775 observed, undefined endogenous fuel substrates are a confounding factor of pathway control,  
776 contributing to the effect of subsequently externally added substrates and inhibitors. In contrast  
777 to the original protocol, an alternative sequence of titration steps is frequently applied, in which  
778 the alternative ‘State 2’ has an entirely different meaning, when this second state is induced by  
779 addition of fuel substrate without ADP (LEAK-state; in contrast to State 2 defined in **Table 1**  
780 as a ROX state), followed by addition of ADP.

781 **State 3** is the state stimulated by addition of fuel substrates while the ADP concentration  
782 is still high (**Table 3**) and supports coupled energy transformation through oxidative  
783 phosphorylation. ‘High ADP’ is a concentration of ADP specifically selected to allow the  
784 measurement of State 3 to State 4 transitions of isolated mitochondria in a closed respirometric  
785 chamber. Repeated ADP titration re-establishes State 3 at ‘high ADP’. Starting at O<sub>2</sub>  
786 concentrations near air-saturation (ca. 200 μM O<sub>2</sub> at sea level and 37 °C), the total ADP  
787 concentration added must be low enough (typically 100 to 300 μM) to allow phosphorylation  
788 to ATP at a coupled O<sub>2</sub> flux that does not lead to O<sub>2</sub> depletion during the transition to State 4.  
789 In contrast, kinetically-saturating ADP concentrations usually are 10-fold higher than ‘high  
790 ADP’, *e.g.*, 2.5 mM in isolated mitochondria. The abbreviation State 3u is occasionally used in  
791 bioenergetics, to indicate the state of respiration after titration of an uncoupler, without  
792 sufficient emphasis on the fundamental difference between OXPHOS-capacity (*well-coupled*  
793 with an *endogenous* uncoupled component) and ET-capacity (*noncoupled*).

794 **State 4** is a LEAK-state that is obtained only if the mitochondrial preparation is intact  
795 and well-coupled. Depletion of ADP by phosphorylation to ATP leads to a decline of O<sub>2</sub> flux  
796 in the transition from State 3 to State 4. Under these conditions of State 4, a maximum  
797 protonmotive force and high ATP/ADP ratio are maintained. For calculation of P<sub>»</sub>/O<sub>2</sub> ratios the  
798 gradual decline of Y<sub>P»/O<sub>2</sub></sub> towards diminishing [ADP] at State 4 must be taken into account  
799 (Gnaiger 2001). State 4 respiration, L<sub>T</sub> (**Table 1**), reflects intrinsic proton leak and intrinsic  
800 ATP hydrolysis activity. O<sub>2</sub> flux in State 4 is an overestimation of LEAK-respiration if the  
801 contaminating ATP hydrolysis activity recycles some ATP to ADP, J<sub>P«</sub>, which stimulates  
802 respiration coupled to phosphorylation, J<sub>P»</sub> > 0. This can be tested by inhibition of the



803 phosphorylation-pathway using oligomycin, ensuring that  $J_{P_{\gg}} = 0$  (State 4o). Alternatively,  
 804 sequential ADP titrations re-establish State 3, followed by State 3 to State 4 transitions while  
 805 sufficient  $O_2$  is available. Anoxia may be reached, however, before exhaustion of ADP (State  
 806 5).

807 **State 5** is the state after exhaustion of  $O_2$  in a closed respirometric chamber. Diffusion of  
 808  $O_2$  from the surroundings into the aqueous solution may be a confounding factor preventing  
 809 complete anoxia (Gnaiger 2001). Chance and Williams (1955) provide an alternative definition  
 810 of State 5, which gives it the different meaning of ROX versus anoxia: ‘State 5 may be obtained  
 811 by antimycin A treatment or by anaerobiosis’.

812 In **Table 3**, only States 3 and 4 (and ‘State 2’ in the alternative protocol: addition of fuel  
 813 substrates without ADP; not included in the table) are coupling control states, with the  
 814 restriction that  $O_2$  flux in State 3 may be limited kinetically by non-saturating ADP  
 815 concentrations (**Table 1**).

816  
817

### 818 3. Normalization: fluxes and flows

819

#### 820 3.1. Normalization: system or sample

821

822 The term *rate* is not sufficiently defined to be useful for reporting data (**Fig. 6**). The  
 823 inconsistency of the meanings of rate becomes fully apparent when considering Galileo  
 824 Galilei’s famous principle, that ‘bodies of different weight all fall at the same rate (have a  
 825 constant acceleration)’ (Coopersmith 2010).

826

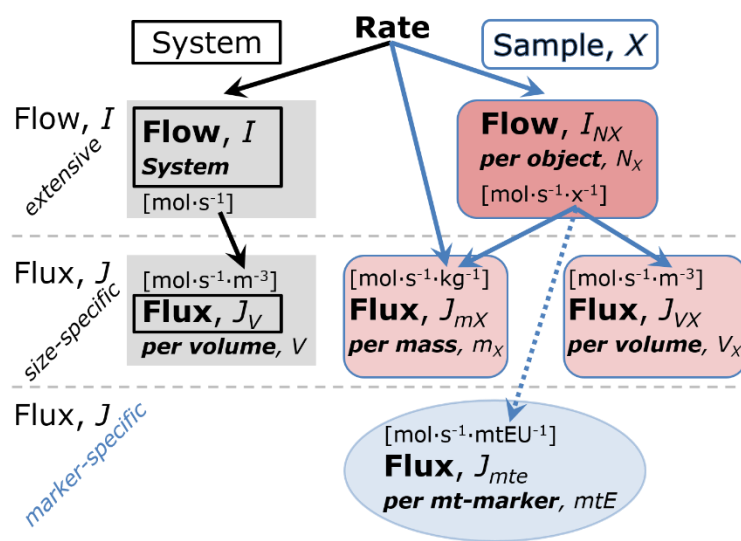
827 **Fig. 6. Different meanings of**  
 828 **rate may lead to confusion, if**  
 829 **the normalization is not**  
 830 **sufficiently specified.** Results are  
 831 frequently expressed as mass-  
 832 specific *flux*,  $J_{mX}$ , per mg protein,  
 833 dry or wet weight (mass). Cell  
 834 volume,  $V_{\text{cell}}$ , may be used for  
 835 normalization (volume-specific  
 836 flux,  $J_{V\text{cell}}$ ), which must be clearly  
 837 distinguished from flow per cell,  
 838  $I_{N\text{cell}}$ , or flux,  $J_V$ , expressed for  
 839 methodological reasons per  
 840 volume of the measurement  
 841 system. For details see **Table 4**.

842

843 **Flow per system,  $I$ :** In a generalization of electrical terms, flow as an extensive quantity  
 844 ( $I$ ; per system) is distinguished from flux as a size-specific quantity ( $J$ ; per system size) (**Fig.**  
 845 **6**). Electric current is flow,  $I_{\text{el}}$  [ $A \equiv C \cdot s^{-1}$ ] per system (extensive quantity). When dividing this  
 846 extensive quantity by system size (cross-sectional area of a ‘wire’), a size-specific quantity is  
 847 obtained, which is flux (current density),  $J_{\text{el}}$  [ $A \cdot m^{-2} = C \cdot s^{-1} \cdot m^{-2}$ ].

848 **Extensive quantities:** An extensive quantity increases proportionally with system size.  
 849 The magnitude of an extensive quantity is completely additive for non-interacting  
 850 subsystems—such as mass or flow expressed per defined system. The magnitude of these  
 851 quantities depends on the extent or size of the system (Cohen *et al.* 2008).

852 **Size-specific quantities:** ‘The adjective *specific* before the name of an extensive quantity  
 853 is often used to mean *divided by mass*’ (Cohen *et al.* 2008). In this system-paradigm, mass-  
 854 specific flux is flow divided by mass of the *system* (the total mass of everything within the



842

855 measuring chamber or reactor). A mass-specific quantity is independent of the extent of non-  
 856 interacting homogenous subsystems. Tissue-specific quantities (related to the *sample* in  
 857 contrast to the *system*) are of fundamental interest in comparative mitochondrial physiology,  
 858 where *specific* refers to the *type of the sample* rather than *mass of the system*. The term *specific*,  
 859 therefore, must be clarified; *sample-specific*, e.g., muscle mass-specific normalization, is  
 860 distinguished from *system-specific* quantities (mass or volume; **Fig. 6**).

861

---

## 862 **Box 2: Metabolic fluxes and flows: vectorial and scalar**

863

864 Fluxes are *vectors*, if they have *spatial* geometric direction in addition to magnitude.  
 865 Electric charge per unit time is electric flow or current,  $I_{el} = dQ_{el} \cdot dt^{-1}$  [A]. When expressed per  
 866 unit cross-sectional area,  $A$  [m<sup>2</sup>], a vector flux is obtained, which is current density or surface-  
 867 density of flow) perpendicular to the direction of flux,  $J_{el} = I_{el} \cdot A^{-1}$  [A·m<sup>-2</sup>] (Cohen et al. 2008).  
 868 For all transformations *flows*,  $I_{tr}$ , are defined as extensive quantities. Vector and scalar *fluxes*  
 869 are obtained as  $J_{tr} = I_{tr} \cdot A^{-1}$  [mol·s<sup>-1</sup>·m<sup>-2</sup>] and  $J_{tr} = I_{tr} \cdot V^{-1}$  [mol·s<sup>-1</sup>·m<sup>-3</sup>], expressing flux as an area-  
 870 specific vector or volume-specific vectorial or scalar quantity, respectively (Gnaiger 1993b).

871 We suggest to define: (1) *vectorial* fluxes, which are translocations as functions of  
 872 *gradients* with direction in geometric space in continuous systems; (2) *vectorial* fluxes, which  
 873 describe translocations in discontinuous systems and are restricted to information on  
 874 *compartmental differences* (**Fig. 2**, transmembrane proton flux); and (3) *scalar* fluxes, which  
 875 are transformations in a *homogenous* system (**Fig. 2**, catabolic O<sub>2</sub> flux,  $J_{kO_2}$ ).

876 Vectorial transmembrane proton fluxes,  $J_{mH^{+}pos}$  and  $J_{mH^{+}neg}$ , are analyzed in a  
 877 heterogenous compartmental system as a quantity with *directional* but not *spatial* information.  
 878 Translocation of protons across the mtIM has a defined direction, either from the negative  
 879 compartment (matrix space; negative, neg-compartment) to the positive compartment (inter-  
 880 membrane space; positive, pos-compartment) or *vice versa* (**Fig. 2**). The arrows defining the  
 881 direction of the translocation between the two compartments may point upwards or downwards,  
 882 right or left, without any implication that these are actual directions in space. The pos-  
 883 compartment is neither above nor below the neg-compartment in a spatial sense, but can be  
 884 visualized arbitrarily in a figure in the upper position (**Fig. 2**). In general, the *compartmental*  
 885 *direction* of vectorial translocation from the neg-compartment to the pos-compartment is  
 886 defined by assigning the initial and final state as *ergodynamic compartments*,  $H^{+}_{neg} \rightarrow H^{+}_{pos}$  or  
 887  $0 = -1 H^{+}_{neg} + 1 H^{+}_{pos}$ , related to work (erg = work) that must be performed to lift the proton from  
 888 a lower to a higher electrochemical potential or from the lower to the higher ergodynamic  
 889 compartment (Gnaiger 1993b).

890 In analogy to *vectorial* translocation, the direction of a *scalar* chemical reaction,  $A \rightarrow B$   
 891 or  $0 = -1 A + 1 B$ , is defined by assigning substrates and products, A and B, as ergodynamic  
 892 compartments. O<sub>2</sub> is defined as a substrate in respiratory O<sub>2</sub> consumption, which together with  
 893 the fuel substrates comprises the substrate compartment of the catabolic reaction (**Fig. 2**).  
 894 Volume-specific scalar O<sub>2</sub> flux is coupled to vectorial translocation, yielding the  $H^{+}_{pos}/O_2$  ratio  
 895 (**Fig. 1**).

896

897

### 898 3.2. Normalization for system-size: flux per chamber volume

899

900 **System-specific flux,  $J_{V,O_2}$ :** The experimental system (experimental chamber) is part of  
 901 the measurement apparatus, separated from the environment as an isolated, closed, open,  
 902 isothermal or non-isothermal system (**Table 4**). On another level, we distinguish between (1)  
 903 the *system* with volume  $V$  and mass  $m$  defined by the system boundaries, and (2) the *sample* or  
 904 *objects* with volume  $V_X$  and mass  $m_X$  which are enclosed in the experimental chamber (**Fig. 6**).  
 905 Metabolic O<sub>2</sub> flow per object,  $I_{O_2/X}$ , increases as the mass of the object is increased. Sample

906 mass-specific O<sub>2</sub> flux,  $J_{O_2/mX}$  should be independent of the mass of the sample studied in the  
 907 instrument chamber, but system volume-specific O<sub>2</sub> flux,  $J_{V,O_2}$  (per volume of the instrument  
 908 chamber), should increase in direct proportion to the mass of the sample in the chamber.  
 909 Whereas  $J_{V,O_2}$  depends on mass-concentration of the sample in the chamber, it should be  
 910 independent of the chamber (system) volume at constant sample mass. There are practical  
 911 limitations to increase the mass-concentration of the sample in the chamber, when one is  
 912 concerned about crowding effects and instrumental time resolution.

913 When the reactor volume does not change during the reaction, which is typical for liquid  
 914 phase reactions, the volume-specific flux of a chemical reaction  $r$  is the time derivative of the  
 915 advancement of the reaction per unit volume,  $J_{V,rB} = d_r\zeta_B/dt \cdot V^{-1}$  [(mol·s<sup>-1</sup>)·L<sup>-1</sup>]. The rate of  
 916 concentration change is  $dc_B/dt$  [(mol·L<sup>-1</sup>)·s<sup>-1</sup>], where concentration is  $c_B = n_B/V$ . There is a  
 917 difference between (1)  $J_{V,rO_2}$  [mol·s<sup>-1</sup>·L<sup>-1</sup>] and (2) rate of concentration change [mol·L<sup>-1</sup>·s<sup>-1</sup>].  
 918 These merge to a single expression only in closed systems. In open systems, external fluxes  
 919 (such as O<sub>2</sub> supply) are distinguished from internal transformations (catabolic flux, O<sub>2</sub>  
 920 consumption). In a closed system, external flows of all substances are zero and O<sub>2</sub> consumption  
 921 (internal flow of catabolic reactions  $k$ ),  $I_{kO_2}$  [pmol·s<sup>-1</sup>], causes a decline of the amount of O<sub>2</sub> in  
 922 the system,  $n_{O_2}$  [nmol]. Normalization of these quantities for the volume of the system,  $V$  [L  $\equiv$   
 923 dm<sup>3</sup>], yields volume-specific O<sub>2</sub> flux,  $J_{V,kO_2} = I_{kO_2}/V$  [nmol·s<sup>-1</sup>·L<sup>-1</sup>], and O<sub>2</sub> concentration, [O<sub>2</sub>]  
 924 or  $c_{O_2} = n_{O_2}/V$  [ $\mu$ mol·L<sup>-1</sup> =  $\mu$ M = nmol·mL<sup>-1</sup>]. Instrumental background O<sub>2</sub> flux is due to external  
 925 flux into a non-ideal closed respirometer; then total volume-specific flux has to be corrected for  
 926 instrumental background O<sub>2</sub> flux—O<sub>2</sub> diffusion into or out of the instrumental chamber.  $J_{V,kO_2}$   
 927 is relevant mainly for methodological reasons and should be compared with the accuracy of  
 928 instrumental resolution of background-corrected flux, e.g.,  $\pm 1$  nmol·s<sup>-1</sup>·L<sup>-1</sup> (Gnaiger 2001).  
 929 ‘Metabolic’ or catabolic indicates O<sub>2</sub> flux,  $J_{kO_2}$ , corrected for: (1) instrumental background O<sub>2</sub>  
 930 flux; (2) chemical background O<sub>2</sub> flux due to autoxidation of chemical components added to  
 931 the incubation medium; and (3)  $R_{ox}$  for O<sub>2</sub>-consuming side reactions unrelated to the catabolic  
 932 pathway  $k$ .

### 933 3.3. Normalization: per sample

934 The challenges of measuring mitochondrial respiratory flux are matched by those of  
 935 normalization. Application of common and defined units is required for direct transfer of  
 936 reported results into a database. The second [s] is the SI unit for the base quantity *time*. It is also  
 937 the standard time-unit used in solution chemical kinetics. A rate may be considered as the  
 938 numerator and normalization as the complementary denominator, which are tightly linked in  
 939 reporting the measurements in a format commensurate with the requirements of a database.  
 940 Normalization (Table 4) is guided by physicochemical principles, methodological  
 941 considerations, and conceptual strategies (Fig. 7).

942 **Sample concentration,  $C_{mX}$ :** Normalization for sample concentration is required to  
 943 report respiratory data. Considering a tissue or cells as the sample,  $X$ , the sample mass is  $m_X$   
 944 [mg], which is frequently measured as wet or dry weight,  $W_w$  or  $W_d$  [mg], or as amount of tissue  
 945 or cell protein,  $m_{\text{Protein}}$ . In the case of permeabilized tissues, cells, and homogenates, the sample  
 946 concentration,  $C_{mX} = m_X/V$  [g·L<sup>-1</sup> = mg·mL<sup>-1</sup>], is the mass of the subsample of tissue that is  
 947 transferred into the instrument chamber.

948 **Mass-specific flux,  $J_{O_2/mX}$ :** Mass-specific flux is obtained by expressing respiration per  
 949 mass of sample,  $m_X$  [mg].  $X$  is the type of sample—isolated mitochondria, tissue homogenate,  
 950 permeabilized fibres or cells. Volume-specific flux is divided by mass concentration of  $X$ ,  $J_{O_2/mX}$   
 951  $= J_{V,O_2}/C_{mX}$ ; or flow per cell is divided by mass per cell,  $J_{O_2/mcell} = I_{O_2/cell}/M_{cell}$ . If mass-specific  
 952 O<sub>2</sub> flux is constant and independent of sample size (expressed as mass), then there is no  
 953 interaction between the subsystems. A 1.5 mg and a 3.0 mg muscle sample respire at identical  
 954 mass-specific flux. Mass-specific O<sub>2</sub> flux, however, may change with the mass of a tissue  
 955

957 sample, cells or isolated mitochondria in the measuring chamber, in which the nature of the  
 958 interaction becomes an issue. Therefore, cell density must be optimized, particularly in  
 959 experiments carried out in wells, considering the confluency of the cell monolayer or clumps  
 960 of cells (Salabei *et al.* 2014).

961 **Number concentration,  $C_{NX}$ :**  $C_{NX}$  is the experimental *number concentration* of sample  
 962  $X$ . In the case of cells or animals, *e.g.*, nematodes,  $C_{NX} = N_X/V [X \cdot L^{-1}]$ , where  $N_X$  is the number  
 963 of cells or organisms in the chamber (**Table 4**).

964  
 965  
 966

**Table 4. Sample concentrations and normalization of flux.**

Expression	Symbol	Definition	Unit	Notes
<b>Sample</b>				
identity of sample	$X$	object: cell, tissue, animal, patient		
number of sample entities $X$	$N_X$	number of objects	x	
mass of sample $X$	$m_X$		kg	1
mass of object $X$	$M_X$	$M_X = m_X \cdot N_X^{-1}$	$kg \cdot x^{-1}$	1
<b>Mitochondria</b>				
Mitochondria	mt	$X = mt$		
amount of mt-elements	$mtE$	quantity of mt-marker	mtEU	
<b>Concentrations</b>				
object number concentration	$C_{NX}$	$C_{NX} = N_X \cdot V^{-1}$	$x \cdot m^{-3}$	2
sample mass concentration	$C_{mX}$	$C_{mX} = m_X \cdot V^{-1}$	$kg \cdot m^{-3}$	
mitochondrial concentration	$C_{mtE}$	$C_{mtE} = mtE \cdot V^{-1}$	$mtEU \cdot m^{-3}$	3
specific mitochondrial density	$D_{mtE}$	$D_{mtE} = mtE \cdot m_X^{-1}$	$mtEU \cdot kg^{-1}$	4
mitochondrial content, $mtE$ per object $X$	$mtE_X$	$mtE_X = mtE \cdot N_X^{-1}$	$mtEU \cdot x^{-1}$	5
<b>O<sub>2</sub> flow and flux</b>				
flow, system	$I_{O_2}$	internal flow	$mol \cdot s^{-1}$	6
volume-specific flux	$J_{V,O_2}$	$J_{V,O_2} = I_{O_2} \cdot V^{-1}$	$mol \cdot s^{-1} \cdot m^{-3}$	7
flow per object $X$	$I_{O_2/X}$	$I_{O_2/X} = J_{V,O_2} \cdot C_{NX}^{-1}$	$mol \cdot s^{-1} \cdot x^{-1}$	8
mass-specific flux	$J_{O_2/mX}$	$J_{O_2/mX} = J_{V,O_2} \cdot C_{mX}^{-1}$	$mol \cdot s^{-1} \cdot kg^{-1}$	9
mitochondria-specific flux	$J_{O_2/mtE}$	$J_{O_2/mtE} = J_{V,O_2} \cdot C_{mtE}^{-1}$	$mol \cdot s^{-1} \cdot mtEU^{-1}$	10

967 1 The SI prefix k is used for the SI base unit of mass ( $kg = 1,000 g$ ). In praxis, various SI prefixes are  
 968 used for convenience, to make numbers easily readable, *e.g.*, 1 mg tissue, cell or mitochondrial mass  
 969 instead of 0.000001 kg.

970 2 In case sample  $X =$  cells, the object number concentration is  $C_{N_{cell}} = N_{cell} \cdot V^{-1}$ , and volume may be  
 971 expressed in [ $dm^3 \equiv L$ ] or [ $cm^3 = mL$ ]. See **Table 5** for different object types.

972 3 mt-concentration is an experimental variable, dependent on sample concentration: (1)  $C_{mtE} = mtE \cdot V^{-1}$ ;  
 973 (2)  $C_{mtE} = mtE_X \cdot C_{NX}$ ; (3)  $C_{mtE} = C_{mX} \cdot D_{mtE}$ .

974 4 If the amount of mitochondria,  $mtE$ , is expressed as mitochondrial mass, then  $D_{mtE}$  is the mass  
 975 fraction of mitochondria in the sample. If  $mtE$  is expressed as mitochondrial volume,  $V_{mt}$ , and the  
 976 mass of sample,  $m_X$ , is replaced by volume of sample,  $V_X$ , then  $D_{mtE}$  is the volume fraction of  
 977 mitochondria in the sample.

978 5  $mtE_X = mtE \cdot N_X^{-1} = C_{mtE} \cdot C_{NX}^{-1}$ .

979 6 O<sub>2</sub> can be replaced by other chemicals B to study different reactions, *e.g.*, ATP, H<sub>2</sub>O<sub>2</sub>, or  
 980 compartmental translocations, *e.g.*, Ca<sup>2+</sup>.

981 7  $I_{O_2}$  and  $V$  are defined per instrument chamber as a system of constant volume (and constant  
 982 temperature), which may be closed or open.  $I_{O_2}$  is abbreviated for  $I_{r,O_2}$ , *i.e.*, the metabolic or internal  
 983 O<sub>2</sub> flow of the chemical reaction  $r$  in which O<sub>2</sub> is consumed, hence the negative stoichiometric  
 984 number,  $\nu_{O_2} = -1$ .  $I_{r,O_2} = d_r n_{O_2} / dt \cdot \nu_{O_2}^{-1}$ . If  $r$  includes all chemical reactions in which O<sub>2</sub> participates, then



- 985  $d_i n_{O_2} = dn_{O_2} - d_e n_{O_2}$ , where  $dn_{O_2}$  is the change in the amount of  $O_2$  in the instrument chamber and  $d_e n_{O_2}$   
 986 is the amount of  $O_2$  added externally to the system. At steady state, by definition  $dn_{O_2} = 0$ , hence  $d_i n_{O_2}$   
 987  $= -d_e n_{O_2}$ .
- 988 8  $J_{V,O_2}$  is an experimental variable, expressed per volume of the instrument chamber.
- 989 9  $I_{O_2/X}$  is a physiological variable, depending on the size of entity  $X$ .
- 990 10 There are many ways to normalize for a mitochondrial marker, that are used in different experimental  
 991 approaches: (1)  $J_{O_2/mtE} = J_{V,O_2} \cdot C_{mtE}^{-1}$ ; (2)  $J_{O_2/mtE} = J_{V,O_2} \cdot C_{mX}^{-1} \cdot D_{mtE}^{-1} = J_{O_2/mX} \cdot D_{mtE}^{-1}$ ; (3)  $J_{O_2/mtE} =$   
 992  $J_{V,O_2} \cdot C_{NX}^{-1} \cdot mtE_X^{-1} = I_{O_2/X} \cdot mtE_X^{-1}$ ; (4)  $J_{O_2/mtE} = I_{O_2} \cdot mtE^{-1}$ . The mt-elemental unit [mtEU] varies between  
 993 different mt-markers.  
 994  
 995

**Table 5. Sample types,  $X$ , abbreviations, and quantification.**

Identity of sample	$X$	$N_X$	Mass <sup>a</sup>	Volume	mt-Marker
mitochondrial preparation	mt-prep	[x]	[kg]	[m <sup>3</sup> ]	[mtEU]
isolated mitochondria	imt		$m_{mt}$	$V_{mt}$	$mtE$
tissue homogenate	thom		$m_{thom}$		$mtE_{thom}$
permeabilized tissue	pti		$m_{pti}$		$mtE_{pti}$
permeabilized fibre	pfi		$m_{pfi}$		$mtE_{pfi}$
permeabilized cell	pce	$N_{pce}$	$M_{pce}$	$V_{pce}$	$mtE_{pce}$
intact cell	ce	$N_{ce}$	$M_{ce}$	$V_{ce}$	$mtE_{ce}$
Organism	org	$N_{org}$	$M_{org}$	$V_{org}$	

996 <sup>a</sup> Instead of mass, frequently the wet weight or dry weight is stated,  $W_w$  or  $W_d$ .  
 997  $m_X$  is mass of the sample [kg],  $M_X$  is mass of the object [kg·x<sup>-1</sup>].  
 998

999 **Flow per object,  $I_{O_2/X}$ :** A special case of normalization is encountered in respiratory  
 1000 studies with permeabilized (or intact) cells. If respiration is expressed per cell, the  $O_2$  flow per  
 1001 measurement system is replaced by the  $O_2$  flow per cell,  $I_{O_2/cell}$  (**Table 4**).  $O_2$  flow can be  
 1002 calculated from volume-specific  $O_2$  flux,  $J_{V,O_2}$  [nmol·s<sup>-1</sup>·L<sup>-1</sup>] (per  $V$  of the measurement chamber  
 1003 [L]), divided by the number concentration of cells,  $C_{Nce} = N_{ce}/V$  [cell·L<sup>-1</sup>], where  $N_{ce}$  is the  
 1004 number of cells in the chamber. Cellular  $O_2$  flow can be compared between cells of identical  
 1005 size. To take into account changes and differences in cell size, normalization is required to  
 1006 obtain cell size-specific or mitochondrial marker-specific  $O_2$  flux (Renner *et al.* 2003).

1007 The complexity changes when the sample is a whole organism studied as an experimental  
 1008 model. The scaling law in respiratory physiology reveals a strong interaction of  $O_2$  flow and  
 1009 individual body mass of an organism, since *basal* metabolic rate (flow) does not increase  
 1010 linearly with body mass, whereas *maximum* mass-specific  $O_2$  flux,  $\dot{V}_{O_2max}$  or  $\dot{V}_{O_2peak}$ , is  
 1011 approximately constant across a large range of individual body mass (Weibel and Hoppeler  
 1012 2005), with individuals, breeds, and species deviating substantially from this relationship.  
 1013  $\dot{V}_{O_2peak}$  of human endurance athletes is 60 to 80 mL  $O_2$ ·min<sup>-1</sup>·kg<sup>-1</sup> body mass, converted to  
 1014  $J_{O_2peak/M}$  of 45 to 60 nmol·s<sup>-1</sup>·g<sup>-1</sup> (Gnaiger 2014; **Table 6**).  
 1015

### 1016 3.4. Normalization for mitochondrial content

1017  
 1018 Tissues can contain multiple cell populations that may have distinct mitochondrial  
 1019 subtypes. Mitochondria undergo dynamic fission and fusion cycles, and can exist in multiple  
 1020 stages and sizes which may be altered by a range of factors. The isolation of mitochondria (often  
 1021 achieved through differential centrifugation) can therefore yield a subsample of the  
 1022 mitochondrial types present in a tissue, depending on isolation protocols utilized (*e.g.*,  
 1023 centrifugation speed). This possible bias should be taken into account when planning  
 1024 experiments using isolated mitochondria. Different sizes of mitochondria are enriched at  
 1025 specific centrifugation speeds, which can be used strategically for isolation of mitochondrial  
 1026 subpopulations.



1027 Part of the mitochondrial content of a tissue is lost during preparation of isolated  
 1028 mitochondria. The fraction of mitochondria in the isolate is expressed as mitochondrial  
 1029 recovery. At a high mitochondrial recovery the sample of isolated mitochondria is more  
 1030 representative of the total mitochondrial population than in preparations characterized by low  
 1031 recovery. Determination of the mitochondrial recovery and yield is based on measurement of  
 1032 the concentration of a mitochondrial marker in the tissue homogenate,  $C_{mtE,thom}$ , which  
 1033 simultaneously provides information on the specific mitochondrial density in the sample.

1034 Normalization is a problematic subject; it is essential to consider the question of the study.  
 1035 If the study aims at comparing tissue performance—such as the effects of a treatment on a  
 1036 specific tissue, then normalization can be successful, using tissue mass or protein content, for  
 1037 example. However, if the aim is to find differences on mitochondrial function independent of  
 1038 mitochondrial density (**Table 4**), then normalization to a mitochondrial marker is imperative  
 1039 (**Fig. 7**). One cannot assume that quantitative changes in various markers—such as  
 1040 mitochondrial proteins—necessarily occur in parallel with one another. It should be established  
 1041 that the marker chosen is not selectively altered by the performed treatment. In conclusion, the  
 1042 normalization must reflect the question under investigation to reach a satisfying answer. On the  
 1043 other hand, the goal of comparing results across projects and institutions requires  
 1044 standardization on normalization for entry into a databank.

1045

<b>Flow, Performance</b>	=	<b>Element function</b>	x	<b>Element density</b>	x	<b>Size of object</b>
$\frac{\text{mol}\cdot\text{s}^{-1}}{x}$	=	$\frac{\text{mol}\cdot\text{s}^{-1}}{x_{mtE}}$	·	$\frac{x_{mtE}}{\text{kg}}$	·	$\frac{\text{kg}}{x}$

<b>A</b>	<b>Flow</b>	=	<b>mt-specific flux</b>	x	<b>mt-structure, functional elements</b>
	$I_{O_2/X}$	=	$J_{O_2/mtE}$	·	$mtE_X$
					$\frac{mtE_X}{M_X} \cdot M_X$

	$I_{O_2/X}$	=	$J_{O_2/mtE}$	·	$D_{mtE}$	·	$M_X$
--	-------------	---	---------------	---	-----------	---	-------

	$\frac{I_{O_2/X}}{M_X}$	=	$\frac{I_{O_2/X}}{mtE_X}$	·	$\frac{mtE_X}{M_X}$
--	-------------------------	---	---------------------------	---	---------------------

<b>B</b>	<b>Flow</b>	=	<b>Object mass- specific flux</b>	x	<b>Mass of object</b>
	$I_{O_2/X}$	=	$J_{O_2/MX}$	·	$M_X$

1046

1047

1048

1049

1050

1051

1052

1053

1054

1055

1056

1057

1058

1059

**Fig. 7. Structure-function analysis of performance of an organism, organ or tissue, or a cell (sample entity, X).  $O_2$  flow,  $I_{O_2/X}$ , is the product of performance per functional element (element function, mitochondria-specific flux), element density (mitochondrial density,  $D_{mtE}$ ), and size of entity X (mass,  $M_X$ ). (A) Structured analysis: performance is the product of mitochondrial function (mt-specific flux) and structure (functional elements;  $D_{mtE}$  times mass of X). (B) Unstructured analysis: performance is the product of entity mass-specific flux,  $J_{O_2/MX} = I_{O_2/X}/M_X = I_{O_2}/m_X$  [ $\text{mol}\cdot\text{s}^{-1}\cdot\text{kg}^{-1}$ ] and size of entity, expressed as mass of X;  $M_X = m_X \cdot N_X^{-1}$  [ $\text{kg}\cdot\text{x}^{-1}$ ]. See **Table 4** for further explanation of quantities and units. Modified from Gnaiger (2014).**

**Mitochondrial concentration,  $C_{mtE}$ , and mitochondrial markers:** Mitochondrial organelles comprise a dynamic cellular reticulum in various states of fusion and fission. Hence, the definition of an "amount" of mitochondria is often misconceived: mitochondria cannot be

1060 counted reliably as a number of occurring elements. Therefore, quantification of the "amount"  
 1061 of mitochondria depends on the measurement of chosen mitochondrial markers. 'Mitochondria  
 1062 are the structural and functional elemental units of cell respiration' (Gnaiger 2014). The  
 1063 quantity of a mitochondrial marker can reflect the amount of *mitochondrial elements*,  $mtE$ ,  
 1064 expressed in various mitochondrial elemental units [mtEU] specific for each measured mt-  
 1065 marker (**Table 4**). However, since mitochondrial quality may change in response to stimuli—  
 1066 particularly in mitochondrial dysfunction and after exercise training (Pesta *et al.* 2011; Campos  
 1067 *et al.* 2017)—some markers can vary while others are unchanged: (1) Mitochondrial volume  
 1068 and membrane area are structural markers, whereas mitochondrial protein mass is frequently  
 1069 used as a marker for isolated mitochondria. (2) Molecular and enzymatic mitochondrial markers  
 1070 (amounts or activities) can be selected as matrix markers, *e.g.*, citrate synthase activity, mtDNA;  
 1071 mtIM-markers, *e.g.*, cytochrome *c* oxidase activity,  $aa_3$  content, cardiolipin, or mtOM-markers,  
 1072 *e.g.*, TOM20. (3) Extending the measurement of mitochondrial marker enzyme activity to  
 1073 mitochondrial pathway capacity, ET- or OXPHOS-capacity can be considered as an integrative  
 1074 functional mitochondrial marker.

1075 Depending on the type of mitochondrial marker, the mitochondrial elements,  $mtE$ , are  
 1076 expressed in marker-specific units. Mitochondrial concentration in the measurement chamber  
 1077 and the tissue of origin are quantified as (1) a quantity for normalization in functional analyses,  
 1078  $C_{mtE}$ , and (2) a physiological output that is the result of mitochondrial biogenesis and  
 1079 degradation,  $D_{mtE}$ , respectively (**Table 4**). It is recommended, therefore, to distinguish  
 1080 *experimental mitochondrial concentration*,  $C_{mtE} = mtE/V$  and *physiological mitochondrial*  
 1081 *density*,  $D_{mtE} = mtE/m_X$ . Then mitochondrial density is the amount of mitochondrial elements  
 1082 per mass of tissue, which is a biological variable (**Fig. 7**). The experimental variable is  
 1083 mitochondrial density multiplied by sample mass concentration in the measuring chamber,  $C_{mtE}$   
 1084  $= D_{mtE} \cdot C_{mX}$ , or mitochondrial content multiplied by sample number concentration,  $C_{mtE} =$   
 1085  $mtE_X \cdot C_{NX}$  (**Table 4**).

1086 **Mitochondria-specific flux,  $J_{O_2/mtE}$** : Volume-specific metabolic  $O_2$  flux depends on: (1)  
 1087 the sample concentration in the volume of the instrument chamber,  $C_{mX}$ , or  $C_{NX}$ ; (2) the  
 1088 mitochondrial density in the sample,  $D_{mtE} = mtE/m_X$  or  $mtE_X = mtE/N_X$ ; and (3) the specific  
 1089 mitochondrial activity or performance per elemental mitochondrial unit,  $J_{O_2/mtE} = J_{V,O_2}/C_{mtE}$   
 1090 [mol·s<sup>-1</sup>·mtEU<sup>-1</sup>] (**Table 4**). Obviously, the numerical results for  $J_{O_2/mtE}$  vary with the type of  
 1091 mitochondrial marker chosen for measurement of  $mtE$  and  $C_{mtE} = mtE/V$  [mtEU·m<sup>-3</sup>].

### 1092 1093 3.5. Evaluation of mitochondrial markers

1094  
1095 Different methods are implicated in the quantification of mitochondrial markers and have  
 1096 different strengths. Some problems are common for all mitochondrial markers,  $mtE$ : (1)  
 1097 Accuracy of measurement is crucial, since even a highly accurate and reproducible  
 1098 measurement of  $O_2$  flux results in an inaccurate and noisy expression normalized for a biased  
 1099 and noisy measurement of a mitochondrial marker. This problem is acute in mitochondrial  
 1100 respiration because the denominators used (the mitochondrial markers) are often small moieties  
 1101 of which accurate and precise determination is difficult. This problem can be avoided when  $O_2$   
 1102 fluxes measured in substrate-uncoupler-inhibitor titration protocols are normalized for flux in  
 1103 a defined respiratory reference state, which is used as an *internal* marker and yields flux control  
 1104 ratios, *FCRs*. *FCRs* are independent of *externally* measured markers and, therefore, are  
 1105 statistically robust, considering the limitations of ratios in general (Jasienski and Bazzaz 1999).  
 1106 *FCRs* indicate qualitative changes of mitochondrial respiratory control, with highest  
 1107 quantitative resolution, separating the effect of mitochondrial density or concentration on  $J_{O_2/mX}$   
 1108 and  $I_{O_2/X}$  from that of function per elemental mitochondrial marker,  $J_{O_2/mtE}$  (Pesta *et al.* 2011;  
 1109 Gnaiger 2014). (2) If mitochondrial quality does not change and only the amount of  
 1110 mitochondria varies as a determinant of mass-specific flux, any marker is equally qualified in

1111 principle; then in practice selection of the optimum marker depends only on the accuracy and  
 1112 precision of measurement of the mitochondrial marker. (3) If mitochondrial flux control ratios  
 1113 change, then there may not be any best mitochondrial marker. In general, measurement of  
 1114 multiple mitochondrial markers enables a comparison and evaluation of normalization for a  
 1115 variety of mitochondrial markers. Particularly during postnatal development, the activity of  
 1116 marker enzymes—such as cytochrome *c* oxidase and citrate synthase—follows different time  
 1117 courses (Drahota *et al.* 2004). Evaluation of mitochondrial markers in healthy controls is  
 1118 insufficient for providing guidelines for application in the diagnosis of pathological states and  
 1119 specific treatments.

1120 In line with the concept of the respiratory control ratio (Chance and Williams 1955a), the  
 1121 most readily used normalization is that of flux control ratios and flux control factors (Gnaiger  
 1122 2014). Selection of the state of maximum flux in a protocol as the reference state has the  
 1123 advantages of: (1) internal normalization; (2) statistical linearization of the response in the range  
 1124 of 0 to 1; and (3) consideration of maximum flux for integrating a large number of elemental  
 1125 steps in the OXPHOS- or ET-pathways. This reduces the risk of selecting a functional marker  
 1126 that is specifically altered by the treatment or pathology, yet increases the chance that the highly  
 1127 integrative pathway is disproportionately affected, *e.g.*, the OXPHOS- rather than ET-pathway  
 1128 in case of an enzymatic defect in the phosphorylation-pathway. In this case, additional  
 1129 information can be obtained by reporting flux control ratios based on a reference state which  
 1130 indicates stable tissue-mass specific flux. Stereological determination of mitochondrial content  
 1131 via two-dimensional transmission electron microscopy can have limitations due to the dynamics  
 1132 of mitochondrial size (Meinild Lundby *et al.* 2017). Accurate determination of three-  
 1133 dimensional volume by two-dimensional microscopy can be both time consuming and  
 1134 statistically challenging (Larsen *et al.* 2012).

1135 The validity of using mitochondrial marker enzymes (citrate synthase activity, Complex  
 1136 I–IV amount or activity) for normalization of flux is limited in part by the same factors that  
 1137 apply to flux control ratios. Strong correlations between various mitochondrial markers and  
 1138 citrate synthase activity (Reichmann *et al.* 1985; Boushel *et al.* 2007; Mogensen *et al.* 2007)  
 1139 are expected in a specific tissue of healthy subjects and in disease states not specifically  
 1140 targeting citrate synthase. Citrate synthase activity is acutely modifiable by exercise  
 1141 (Tonkonogi *et al.* 1997; Leek *et al.* 2001). Evaluation of mitochondrial markers related to a  
 1142 selected age and sex cohort cannot be extrapolated to provide recommendations for  
 1143 normalization in respirometric diagnosis of disease, in different states of development and  
 1144 ageing, different cell types, tissues, and species. mtDNA normalized to nDNA via qPCR is  
 1145 correlated to functional mitochondrial markers including OXPHOS- and ET-capacity in some  
 1146 cases (Puntschart *et al.* 1995; Wang *et al.* 1999; Menshikova *et al.* 2006; Boushel *et al.* 2007),  
 1147 but lack of such correlations have been reported (Menshikova *et al.* 2005; Schultz and Wiesner  
 1148 2000; Pesta *et al.* 2011). Several studies indicate a strong correlation between cardiolipin  
 1149 content and increase in mitochondrial function with exercise (Menshikova *et al.* 2005;  
 1150 Menshikova *et al.* 2007; Larsen *et al.* 2012; Faber *et al.* 2014), but its use as a general  
 1151 mitochondrial biomarker in disease remains questionable.

1152

### 1153 3.6. Conversion: units

1154

1155 Many different units have been used to report the O<sub>2</sub> consumption rate, OCR (**Table 6**).  
 1156 *SI* base units provide the common reference to introduce the theoretical principles (**Fig. 6**), and  
 1157 are used with appropriately chosen *SI* prefixes to express numerical data in the most practical  
 1158 format, with an effort towards unification within specific areas of application (**Table 7**).  
 1159 Reporting data in *SI* units—including the mole [mol], coulomb [C], joule [J], and second [s]—  
 1160 should be encouraged, particularly by journals which propose the use of *SI* units.

1161 Although volume is expressed as  $\text{m}^3$  using the *SI* base unit, the litre [ $\text{dm}^3$ ] is a  
 1162 conventional unit of volume for concentration and is used for most solution chemical kinetics.  
 1163 If one multiplies  $I_{\text{O}_2/\text{cell}}$  by  $C_{\text{Ncell}}$ , then the result will not only be the amount of  $\text{O}_2$  [mol]  
 1164 consumed per time [ $\text{s}^{-1}$ ] in one litre [ $\text{L}^{-1}$ ], but also the change in  $\text{O}_2$  concentration per second  
 1165 (for any volume of an ideally closed system). This is ideal for kinetic modeling as it blends with  
 1166 chemical rate equations where concentrations are typically expressed in  $\text{mol}\cdot\text{L}^{-1}$  (Wagner *et al.*  
 1167 2011). In studies of multinuclear cells—such as differentiated skeletal muscle cells—it is easy  
 1168 to determine the number of nuclei but not the total number of cells. A generalized concept,  
 1169 therefore, is obtained by substituting cells by nuclei as the sample entity. This does not hold,  
 1170 however, for enucleated platelets.

1171

1172 **Table 6. Conversion of various units used in respirometry and**  
 1173 **ergometry.**  $e^-$  is the number of electrons or reducing equivalents.  $z_B$  is the  
 1174 charge number of entity B.

1175

1 Unit	x	Multiplication factor	<i>SI</i> -unit	Note
ng.atom $\text{O}\cdot\text{s}^{-1}$	(2 $e^-$ )	0.5	nmol $\text{O}_2\cdot\text{s}^{-1}$	
ng.atom $\text{O}\cdot\text{min}^{-1}$	(2 $e^-$ )	8.33	pmol $\text{O}_2\cdot\text{s}^{-1}$	
natom $\text{O}\cdot\text{min}^{-1}$	(2 $e^-$ )	8.33	pmol $\text{O}_2\cdot\text{s}^{-1}$	
nmol $\text{O}_2\cdot\text{min}^{-1}$	(4 $e^-$ )	16.67	pmol $\text{O}_2\cdot\text{s}^{-1}$	
nmol $\text{O}_2\cdot\text{h}^{-1}$	(4 $e^-$ )	0.2778	pmol $\text{O}_2\cdot\text{s}^{-1}$	
mL $\text{O}_2\cdot\text{min}^{-1}$ at STPD <sup>a</sup>		0.744	$\mu\text{mol O}_2\cdot\text{s}^{-1}$	1
W = J/s at -470 kJ/mol $\text{O}_2$		-2.128	$\mu\text{mol O}_2\cdot\text{s}^{-1}$	
mA = mC $\cdot\text{s}^{-1}$	( $z_{\text{H}^+} = 1$ )	10.36	nmol $\text{H}^+\cdot\text{s}^{-1}$	2
mA = mC $\cdot\text{s}^{-1}$	( $z_{\text{O}_2} = 4$ )	2.59	nmol $\text{O}_2\cdot\text{s}^{-1}$	2
nmol $\text{H}^+\cdot\text{s}^{-1}$	( $z_{\text{H}^+} = 1$ )	0.09649	mA	3
nmol $\text{O}_2\cdot\text{s}^{-1}$	( $z_{\text{O}_2} = 4$ )	0.38594	mA	3

1176 1 At standard temperature and pressure dry (STPD:  $0\text{ }^\circ\text{C} = 273.15\text{ K}$  and  $1\text{ atm} =$   
 1177  $101.325\text{ kPa} = 760\text{ mmHg}$ ), the molar volume of an ideal gas,  $V_m$ , and  $V_{m,\text{O}_2}$  is  
 1178  $22.414$  and  $22.392\text{ L}\cdot\text{mol}^{-1}$ , respectively. Rounded to three decimal places, both  
 1179 values yield the conversion factor of  $0.744$ . For comparison at NTPD ( $20\text{ }^\circ\text{C}$ ),  
 1180  $V_{m,\text{O}_2}$  is  $24.038\text{ L}\cdot\text{mol}^{-1}$ . Note that the *SI* standard pressure is  $100\text{ kPa}$ .

1181 2 The multiplication factor is  $10^6/(z_B\cdot F)$ .

1182 3 The multiplication factor is  $z_B\cdot F/10^6$ .

1183

1184 For studies of cells, we recommend that respiration be expressed, as far as possible, as:  
 1185 (1)  $\text{O}_2$  flux normalized for a mitochondrial marker, for separation of the effects of mitochondrial  
 1186 quality and content on cell respiration (this includes *FCRs* as a normalization for a functional  
 1187 mitochondrial marker); (2)  $\text{O}_2$  flux in units of cell volume or mass, for comparison of respiration  
 1188 of cells with different cell size (Renner *et al.* 2003) and with studies on tissue preparations, and  
 1189 (3)  $\text{O}_2$  flow in units of attomole ( $10^{-18}\text{ mol}$ ) of  $\text{O}_2$  consumed in a second by each cell  
 1190 [ $\text{amol}\cdot\text{s}^{-1}\cdot\text{cell}^{-1}$ ], numerically equivalent to [ $\text{pmol}\cdot\text{s}^{-1}\cdot 10^{-6}\text{ cells}$ ]. This convention allows  
 1191 information to be easily used when designing experiments in which  $\text{O}_2$  flow must be considered.  
 1192 For example, to estimate the volume-specific  $\text{O}_2$  flux in an instrument chamber that would be  
 1193 expected at a particular cell number concentration, one simply needs to multiply the flow per  
 1194 cell by the number of cells per volume of interest. This provides the amount of  $\text{O}_2$  [mol]  
 1195 consumed per time [ $\text{s}^{-1}$ ] per unit volume [ $\text{L}^{-1}$ ]. At an  $\text{O}_2$  flow of  $100\text{ amol}\cdot\text{s}^{-1}\cdot\text{cell}^{-1}$  and a cell  
 1196 density of  $10^9\text{ cells}\cdot\text{L}^{-1}$  ( $10^6\text{ cells}\cdot\text{mL}^{-1}$ ), the volume-specific  $\text{O}_2$  flux is  $100\text{ nmol}\cdot\text{s}^{-1}\cdot\text{L}^{-1}$  ( $100$   
 1197  $\text{pmol}\cdot\text{s}^{-1}\cdot\text{mL}^{-1}$ ).

1198 ET-capacity in human cell types including HEK 293, primary HUVEC and fibroblasts  
 1199 ranges from 50 to 180  $\text{amol}\cdot\text{s}^{-1}\cdot\text{cell}^{-1}$ , measured in intact cells in the noncoupled state (see  
 1200 Gnaiger 2014). At 100  $\text{amol}\cdot\text{s}^{-1}\cdot\text{cell}^{-1}$  corrected for *Rox*, the current across the mt-membranes,  
 1201  $I_{H^+e}$ , approximates 193  $\text{pA}\cdot\text{cell}^{-1}$  or 0.2 nA per cell. See Rich (2003) for an extension of  
 1202 quantitative bioenergetics from the molecular to the human scale, with a transmembrane proton  
 1203 flux equivalent to 520 A in an adult at a catabolic power of -110 W. Modelling approaches  
 1204 illustrate the link between protonmotive force and currents (Willis *et al.* 2016).  
 1205  
 1206 **Table 7. Conversion of units with preservation of numerical values.**

Name	Frequently used unit	Equivalent unit	Note
volume-specific flux, $J_{V,O_2}$	$\text{pmol}\cdot\text{s}^{-1}\cdot\text{mL}^{-1}$	$\text{nmol}\cdot\text{s}^{-1}\cdot\text{L}^{-1}$	1
	$\text{mmol}\cdot\text{s}^{-1}\cdot\text{L}^{-1}$	$\text{mol}\cdot\text{s}^{-1}\cdot\text{m}^{-3}$	
cell-specific flow, $I_{O_2/\text{cell}}$	$\text{pmol}\cdot\text{s}^{-1}\cdot 10^{-6}$ cells	$\text{amol}\cdot\text{s}^{-1}\cdot\text{cell}^{-1}$	2
	$\text{pmol}\cdot\text{s}^{-1}\cdot 10^{-9}$ cells	$\text{zmol}\cdot\text{s}^{-1}\cdot\text{cell}^{-1}$	3
cell number concentration, $C_{Nce}$	$10^6$ cells $\cdot\text{mL}^{-1}$	$10^9$ cells $\cdot\text{L}^{-1}$	
mitochondrial protein concentration, $C_{mtE}$	$0.1$ mg $\cdot\text{mL}^{-1}$	$0.1$ g $\cdot\text{L}^{-1}$	
mass-specific flux, $J_{O_2/m}$	$\text{pmol}\cdot\text{s}^{-1}\cdot\text{mg}^{-1}$	$\text{nmol}\cdot\text{s}^{-1}\cdot\text{g}^{-1}$	4
catabolic power, $P_k$	$\mu\text{W}\cdot 10^{-6}$ cells	$\text{pW}\cdot\text{cell}^{-1}$	1
Volume	1,000 L	$\text{m}^3$ (1,000 kg)	
	L	$\text{dm}^3$ (kg)	
	mL	$\text{cm}^3$ (g)	
	$\mu\text{L}$	$\text{mm}^3$ (mg)	
	fL	$\mu\text{m}^3$ (pg)	5
amount of substance concentration	$\text{M} = \text{mol}\cdot\text{L}^{-1}$	$\text{mol}\cdot\text{dm}^{-3}$	

1207  
 1208 1 pmol: picomole =  $10^{-12}$  mol                      4 nmol: nanomole =  $10^{-9}$  mol  
 1209 2 amol: attomole =  $10^{-18}$  mol                      5 fL: femtolitre =  $10^{-15}$  L  
 1210 3 zmol: zeptomole =  $10^{-21}$  mol

1211  
 1212 We consider isolated mitochondria as powerhouses and proton pumps as molecular  
 1213 machines to relate experimental results to energy metabolism of the intact cell. The cellular  
 1214  $P_{\gg}/O_2$  based on oxidation of glycogen is increased by the glycolytic (fermentative) substrate-  
 1215 level phosphorylation of 3  $P_{\gg}/\text{Glyc}$  or 0.5 mol  $P_{\gg}$  for each mol  $O_2$  consumed in the complete  
 1216 oxidation of a mol glycosyl unit (Glyc). Adding 0.5 to the mitochondrial  $P_{\gg}/O_2$  ratio of 5.4  
 1217 yields a bioenergetic cell physiological  $P_{\gg}/O_2$  ratio close to 6. Two NADH equivalents are  
 1218 formed during glycolysis and transported from the cytosol into the mitochondrial matrix, either  
 1219 by the malate-aspartate shuttle or by the glycerophosphate shuttle resulting in different  
 1220 theoretical yields of ATP generated by mitochondria, the energetic cost of which potentially  
 1221 must be taken into account. Considering also substrate-level phosphorylation in the TCA cycle,  
 1222 this high  $P_{\gg}/O_2$  ratio not only reflects proton translocation and OXPHOS studied in isolation,  
 1223 but integrates mitochondrial physiology with energy transformation in the living cell (Gnaiger  
 1224 1993a).

#### 1225 1226 1227 **4. Conclusions**

1228  
 1229 MitoEAGLE can serve as a gateway to better diagnose mitochondrial respiratory defects  
 1230 linked to genetic variation, age-related health risks, sex-specific mitochondrial performance,  
 1231 lifestyle with its effects on degenerative diseases, and thermal and chemical environment. The



1232 present recommendations on coupling control states and rates, linked to the concept of the  
 1233 protonmotive force, are focused on studies with mitochondrial preparations. These will be  
 1234 extended in a series of reports on pathway control of mitochondrial respiration, respiratory  
 1235 states in intact cells, and harmonization of experimental procedures.

1236 The optimal choice for expressing mitochondrial and cell respiration (**Box 3**) as O<sub>2</sub> flow  
 1237 per biological system, and normalization for specific tissue-markers (volume, mass, protein)  
 1238 and mitochondrial markers (volume, protein, content, mtDNA, activity of marker enzymes,  
 1239 respiratory reference state) is guided by the scientific question under study. Interpretation of  
 1240 the obtained data depends critically on appropriate normalization, and therefore reporting rates  
 1241 merely as nmol·s<sup>-1</sup> is discouraged, since it restricts the analysis to intra-experimental  
 1242 comparison of relative (qualitative) differences. Expressing O<sub>2</sub> flow per cell may not be possible  
 1243 when dealing with tissues. For studies with mitochondrial preparations, we recommend that  
 1244 normalizations be provided as far as possible: (1) on a per cell basis as O<sub>2</sub> flow (a biophysical  
 1245 normalization); (2) per g cell or tissue protein, or per cell or tissue mass as mass-specific O<sub>2</sub>  
 1246 flux (a cellular normalization); and (3) per mitochondrial marker as mt-specific flux (a  
 1247 mitochondrial normalization). With information on cell size and the use of multiple  
 1248 normalizations, maximum potential information is available (Renner *et al.* 2003; Wagner *et al.*  
 1249 2011; Gnaiger 2014).

1250 Total mitochondrial protein is frequently applied as a mitochondrial marker restricted to  
 1251 isolated mitochondria. The mitochondrial recovery and yield, and experimental criteria for  
 1252 evaluation of purity versus integrity should be reported. Mitochondrial markers—such as citrate  
 1253 synthase activity as an enzymatic matrix marker—provide a link to the tissue of origin on the  
 1254 basis of calculating the mitochondrial recovery, *i.e.*, the fraction of mitochondrial marker  
 1255 obtained from a unit mass of tissue.

1256

---

### 1257 **Box 3: Mitochondrial and cell respiration**

1258

1259 Mitochondrial and cell respiration is the process of exergonic and exothermic energy  
 1260 transformation in which scalar redox reactions are coupled to vectorial ion translocation across  
 1261 a semipermeable membrane, which separates the small volume of a bacterial cell or  
 1262 mitochondrion from the larger volume of its surroundings. The electrochemical exergy can be  
 1263 partially conserved in the phosphorylation of ADP to ATP or in ion pumping, or dissipated in  
 1264 an electrochemical short-circuit. Respiration is thus clearly distinguished from fermentation as  
 1265 the counterpart of cellular core energy metabolism. Respiration is separated in mitochondrial  
 1266 preparations from the partial contribution of fermentative pathways of the intact cell. Residual  
 1267 O<sub>2</sub> consumption—as measured after inhibition of mitochondrial electron transfer—does not  
 1268 belong to the class of catabolic reactions and is, therefore, subtracted from total O<sub>2</sub> consumption  
 1269 to obtain baseline-corrected respiration.

---

1270

1271 Terms and symbols are summarized in **Table 8**. Their use will facilitate transdisciplinary  
 1272 communication and support further developments towards a consistent theory of bioenergetics  
 1273 and mitochondrial physiology. Technical terms related to and defined with normal words can  
 1274 be used as index terms in databases, support the creation of ontologies towards semantic  
 1275 information processing (MitoPedia), and help in communicating analytical findings as  
 1276 impactful data-driven stories. *‘Making data available without making it understandable may be  
 1277 worse than not making it available at all’* (National Academies of Sciences, Engineering, and  
 1278 Medicine 2018). This is a call to carefully contribute to FAIR principles (Findable, Accessible,  
 1279 Interoperable, Reusable) for the sharing of scientific data.

1280

1281

1282

**Table 8. Terms, symbols, and units.**

Term	Symbol	Unit	Links and comments
alternative quinol oxidase	AOX		Fig. 1
amount of substance B	$n_B$	[mol]	
Complexes I to IV	CI to CIV		respiratory ET Complexes; Fig. 1
concentration of substance B	$c_B = n_B \cdot V^{-1}$ ; [B]	[mol·m <sup>-3</sup> ]	Box 2
electron transfer system	ETS		Fig. 1, Fig. 4
flow, for substance B	$I_B$	[mol·s <sup>-1</sup> ]	system-related extensive quantity; Fig. 6
flux, for substance B	$J_B$	<i>varies</i>	size-specific quantity; Fig. 6
inorganic phosphate	$P_i$		Fig. 2
LEAK	LEAK		Tab. 1, Fig. 4
mass of sample X	$m_X$	[kg]	Tab. 4
mass of entity X	$M_X$	[kg]	mass of object X; Tab. 4
MITOCARTA			<a href="https://www.broadinstitute.org/scientific-community/science/programs/metabolic-disease-program/publications/mitocarta/mitocarta-in-0">https://www.broadinstitute.org/scientific-community/science/programs/metabolic-disease-program/publications/mitocarta/mitocarta-in-0</a>
MitoPedia			<a href="http://www.bioblast.at/index.php/MitoPedia">http://www.bioblast.at/index.php/MitoPedia</a>
mitochondria or mitochondrial	mt		Box 1
mitochondrial DNA	mtDNA		Box 1
mitochondrial concentration	$C_{mtE} = mtE \cdot V^{-1}$	[mtEU·m <sup>-3</sup> ]	Tab. 4
mitochondrial content	$mtE_X = mtE \cdot N_X^{-1}$	[mtEU·x <sup>-1</sup> ]	Tab. 4
mitochondrial elemental unit	mtEU	<i>varies</i>	Tab. 4, specific units for mt-marker
mitochondrial inner membrane	mtIM		MIM is widely used; the first M is replaced by mt; Box 1
mitochondrial outer membrane	mtOM		MOM is widely used; the first M is replaced by mt; Box 1
mitochondrial recovery	$Y_{mtE}$		fraction of <i>mtE</i> recovered in sample from the tissue of origin
mitochondrial yield	$Y_{mtE/m}$		$Y_{mtE/m} = Y_{mtE} \cdot D_{mtE}$
negative	neg		Fig. 2
number concentration of X	$C_{NX}$	[x·m <sup>-3</sup> ]	Tab. 4
number of entities X	$N_X$	[x]	Tab. 4, Fig. 7
number of entity B	$N_B$	[x]	Tab. 4
oxidative phosphorylation	OXPPOS		Tab. 1, Fig. 4
oxygen concentration	$c_{O_2} = n_{O_2} \cdot V^{-1}$ ; [O <sub>2</sub> ]	[mol·m <sup>-3</sup> ]	Section 3.2
phosphorylation of ADP to ATP	P»		Section 2.2
positive	pos		Fig. 2
proton in the negative compartment	$H^{+}_{neg}$		Fig. 2
proton in the positive compartment	$H^{+}_{pos}$		Fig. 2
rate of electron transfer in ET state	$E$		ET-capacity; Tab. 1
rate of LEAK respiration	$L$		Tab. 1
rate of oxidative phosphorylation	$P$		OXPPOS capacity; Tab. 1
rate of residual oxygen consumption	$ROX$		Tab. 1
residual oxygen consumption	ROX		Tab. 1
specific mitochondrial density	$D_{mtE} = mtE \cdot m_X^{-1}$	[mtEU·kg <sup>-1</sup> ]	Tab. 7
volume	$V$	[m <sup>3</sup> ]	
weight, dry weight	$W_d$	[kg]	used as mass of sample X; Fig. 6
weight, wet weight	$W_w$	[kg]	used as mass of sample X; Fig. 6

**Acknowledgements**

We thank M. Beno for management assistance. Supported by COST Action CA15203 MitoEAGLE and K-Regio project MitoFit (E.G.).

1344 **Competing financial interests:** E.G. is founder and CEO of Oroboros Instruments, Innsbruck,  
1345 Austria.

1346  
1347

## 1348 5. References

- 1349  
1350 Altmann R (1894) Die Elementarorganismen und ihre Beziehungen zu den Zellen. Zweite vermehrte Auflage.  
1351 Verlag Von Veit & Comp, Leipzig:160 pp.
- 1352 Beard DA (2005) A biophysical model of the mitochondrial respiratory system and oxidative phosphorylation.  
1353 PLoS Comput Biol 1(4):e36.
- 1354 Benda C (1898) Weitere Mitteilungen über die Mitochondria. Verh Dtsch Physiol Ges:376-83.
- 1355 Birkedal R, Laasmaa M, Vendelin M (2014) The location of energetic compartments affects energetic  
1356 communication in cardiomyocytes. Front Physiol 5:376.
- 1357 Breton S, Beaupré HD, Stewart DT, Hoeh WR, Blier PU (2007) The unusual system of doubly uniparental  
1358 inheritance of mtDNA: isn't one enough? Trends Genet 23:465-74.
- 1359 Brown GC (1992) Control of respiration and ATP synthesis in mammalian mitochondria and cells. Biochem J  
1360 284:1-13.
- 1361 Calvo SE, Klauser CR, Mootha VK (2016) MitoCarta2.0: an updated inventory of mammalian mitochondrial  
1362 proteins. Nucleic Acids Research 44:D1251-7.
- 1363 Calvo SE, Julien O, Clauser KR, Shen H, Kamer KJ, Wells JA, Mootha VK (2017) Comparative analysis of  
1364 mitochondrial N-termini from mouse, human, and yeast. Mol Cell Proteomics 16:512-23.
- 1365 Campos JC, Queliconi BB, Bozi LHM, Bechara LRG, Dourado PMM, Andres AM, Jannig PR, Gomes KMS,  
1366 Zambelli VO, Rocha-Resende C, Guatimosim S, Brum PC, Mochly-Rosen D, Gottlieb RA, Kowaltowski AJ,  
1367 Ferreira JCB (2017) Exercise reestablishes autophagic flux and mitochondrial quality control in heart failure.  
1368 Autophagy 13:1304-317.
- 1369 Canton M, Luvisetto S, Schmehl I, Azzone GF (1995) The nature of mitochondrial respiration and  
1370 discrimination between membrane and pump properties. Biochem J 310:477-81.
- 1371 Chance B, Williams GR (1955a) Respiratory enzymes in oxidative phosphorylation. I. Kinetics of oxygen  
1372 utilization. J Biol Chem 217:383-93.
- 1373 Chance B, Williams GR (1955b) Respiratory enzymes in oxidative phosphorylation: III. The steady state. J Biol  
1374 Chem 217:409-27.
- 1375 Chance B, Williams GR (1955c) Respiratory enzymes in oxidative phosphorylation. IV. The respiratory chain. J  
1376 Biol Chem 217:429-38.
- 1377 Chance B, Williams GR (1956) The respiratory chain and oxidative phosphorylation. Adv Enzymol Relat Subj  
1378 Biochem 17:65-134.
- 1379 Cobb LJ, Lee C, Xiao J, Yen K, Wong RG, Nakamura HK, Mehta HH, Gao Q, Ashur C, Huffman DM, Wan J,  
1380 Muzumdar R, Barzilai N, Cohen P (2016) Naturally occurring mitochondrial-derived peptides are age-  
1381 dependent regulators of apoptosis, insulin sensitivity, and inflammatory markers. Aging (Albany NY) 8:796-  
1382 809.
- 1383 Cohen ER, Cvitas T, Frey JG, Holmström B, Kuchitsu K, Marquardt R, Mills I, Pavese F, Quack M, Stohner J,  
1384 Strauss HL, Takami M, Thor HL (2008) Quantities, units and symbols in physical chemistry, IUPAC Green  
1385 Book, 3rd Edition, 2nd Printing, IUPAC & RSC Publishing, Cambridge.
- 1386 Cooper H, Hedges LV, Valentine JC, eds (2009) The handbook of research synthesis and meta-analysis. Russell  
1387 Sage Foundation.
- 1388 Coopersmith J (2010) Energy, the subtle concept. The discovery of Feynman's blocks from Leibnitz to Einstein.  
1389 Oxford University Press:400 pp.
- 1390 Cummins J (1998) Mitochondrial DNA in mammalian reproduction. Rev Reprod 3:172-82.
- 1391 Dai Q, Shah AA, Garde RV, Yonish BA, Zhang L, Medvitz NA, Miller SE, Hansen EL, Dunn CN, Price TM  
1392 (2013) A truncated progesterone receptor (PR-M) localizes to the mitochondrion and controls cellular  
1393 respiration. Mol Endocrinol 27:741-53.
- 1394 Divakaruni AS, Brand MD (2011) The regulation and physiology of mitochondrial proton leak. Physiology  
1395 (Bethesda) 26:192-205.
- 1396 Doerrier C, Garcia-Souza LF, Krumschnabel G, Wohlfarter Y, Mészáros AT, Gnaiger E (2018) High-Resolution  
1397 Fluorescence Respirometry and OXPHOS protocols for human cells, permeabilized fibres from small biopsies of  
1398 muscle and isolated mitochondria. Methods Mol. Biol. (in press)
- 1399 Doskey CM, van 't Erve TJ, Wagner BA, Buettner GR (2015) Moles of a substance per cell is a highly  
1400 informative dosing metric in cell culture. PLOS ONE 10:e0132572.
- 1401 Drahota Z, Milerová M, Stieglerová A, Houstek J, Ostádal B (2004) Developmental changes of cytochrome c  
1402 oxidase and citrate synthase in rat heart homogenate. Physiol Res 53:119-22.
- 1403 Duarte FV, Palmeira CM, Rolo AP (2014) The role of microRNAs in mitochondria: small players acting wide.  
1404 Genes (Basel) 5:865-86.

- 1405 Ernster L, Schatz G (1981) Mitochondria: a historical review. *J Cell Biol* 91:227s-55s.
- 1406 Estabrook RW (1967) Mitochondrial respiratory control and the polarographic measurement of ADP:O ratios. *Methods Enzymol* 10:41-7.
- 1407
- 1408 Faber C, Zhu ZJ, Castellino S, Wagner DS, Brown RH, Peterson RA, Gates L, Barton J, Bickett M, Hagerty L,  
1409 Kimbrough C, Sola M, Bailey D, Jordan H, Elangbam CS (2014) Cardiolipin profiles as a potential  
1410 biomarker of mitochondrial health in diet-induced obese mice subjected to exercise, diet-restriction and  
1411 ephedrine treatment. *J Appl Toxicol* 34:1122-9.
- 1412 Fell D (1997) Understanding the control of metabolism. Portland Press.
- 1413 Garlid KD, Beavis AD, Ratkje SK (1989) On the nature of ion leaks in energy-transducing membranes. *Biochim*  
1414 *Biophys Acta* 976:109-20.
- 1415 Garlid KD, Semrad C, Zinchenko V. Does redox slip contribute significantly to mitochondrial respiration? In:  
1416 Schuster S, Rigoulet M, Ouhabi R, Mazat J-P, eds (1993) Modern trends in biothermokinetics. Plenum Press,  
1417 New York, London:287-93.
- 1418 Gerö D, Szabo C (2016) Glucocorticoids suppress mitochondrial oxidant production via upregulation of  
1419 uncoupling protein 2 in hyperglycemic endothelial cells. *PLoS One* 11:e0154813.
- 1420 Gnaiger E. Efficiency and power strategies under hypoxia. Is low efficiency at high glycolytic ATP production a  
1421 paradox? In: Surviving Hypoxia: Mechanisms of Control and Adaptation. Hochachka PW, Lutz PL, Sick T,  
1422 Rosenthal M, Van den Thillart G, eds (1993a) CRC Press, Boca Raton, Ann Arbor, London, Tokyo:77-109.
- 1423 Gnaiger E (1993b) Nonequilibrium thermodynamics of energy transformations. *Pure Appl Chem* 65:1983-2002.
- 1424 Gnaiger E (2001) Bioenergetics at low oxygen: dependence of respiration and phosphorylation on oxygen and  
1425 adenosine diphosphate supply. *Respir Physiol* 128:277-97.
- 1426 Gnaiger E (2009) Capacity of oxidative phosphorylation in human skeletal muscle. New perspectives of  
1427 mitochondrial physiology. *Int J Biochem Cell Biol* 41:1837-45.
- 1428 Gnaiger E (2014) Mitochondrial pathways and respiratory control. An introduction to OXPHOS analysis. 4th ed.  
1429 *Mitochondr Physiol Network* 19.12. Oroboros MiPNet Publications, Innsbruck:80 pp.
- 1430 Gnaiger E, Méndez G, Hand SC (2000) High phosphorylation efficiency and depression of uncoupled respiration  
1431 in mitochondria under hypoxia. *Proc Natl Acad Sci USA* 97:11080-5.
- 1432 Greggio C, Jha P, Kulkarni SS, Lagarrigue S, Broskey NT, Boutant M, Wang X, Conde Alonso S, Ofori E,  
1433 Auwerx J, Cantó C, Amati F (2017) Enhanced respiratory chain supercomplex formation in response to  
1434 exercise in human skeletal muscle. *Cell Metab* 25:301-11.
- 1435 Hinkle PC (2005) P/O ratios of mitochondrial oxidative phosphorylation. *Biochim Biophys Acta* 1706:1-11.
- 1436 Hofstadter DR (1979) Gödel, Escher, Bach: An eternal golden braid. A metaphorical fugue on minds and  
1437 machines in the spirit of Lewis Carroll. Harvester Press:499 pp.
- 1438 Illaste A, Laasmaa M, Peterson P, Vendelin M (2012) Analysis of molecular movement reveals latticelike  
1439 obstructions to diffusion in heart muscle cells. *Biophys J* 102:739-48.
- 1440 Jasienski N, Bazzaz FA (1999) The fallacy of ratios and the testability of models in biology. *Oikos* 84:321-26.
- 1441 Jepihhina N, Beraud N, Sepp M, Birkedal R, Vendelin M (2011) Permeabilized rat cardiomyocyte response  
1442 demonstrates intracellular origin of diffusion obstacles. *Biophys J* 101:2112-21.
- 1443 Klepinin A, Ounpuu L, Guzun R, Chekulayev V, Timohhina N, Tepp K, Shevchuk I, Schlattner U, Kaambre T  
1444 (2016) Simple oxygraphic analysis for the presence of adenylate kinase 1 and 2 in normal and tumor cells. *J*  
1445 *Bioenerg Biomembr* 48:531-48.
- 1446 Klingenberg M (2017) UCP1 - A sophisticated energy valve. *Biochimie* 134:19-27.
- 1447 Koit A, Shevchuk I, Ounpuu L, Klepinin A, Chekulayev V, Timohhina N, Tepp K, Puurand M, Truu L, Heck K,  
1448 Valvere V, Guzun R, Kaambre T (2017) Mitochondrial respiration in human colorectal and breast cancer  
1449 clinical material is regulated differently. *Oxid Med Cell Longev* 1372640.
- 1450 Komlódi T, Tretter L (2017) Methylene blue stimulates substrate-level phosphorylation catalysed by succinyl-  
1451 CoA ligase in the citric acid cycle. *Neuropharmacology* 123:287-98.
- 1452 Lane N (2005) Power, sex, suicide: mitochondria and the meaning of life. Oxford University Press:354 pp.
- 1453 Larsen S, Nielsen J, Neigaard Nielsen C, Nielsen LB, Wibrand F, Stride N, Schroder HD, Boushel RC, Helge  
1454 JW, Dela F, Hey-Mogensen M (2012) Biomarkers of mitochondrial content in skeletal muscle of healthy  
1455 young human subjects. *J Physiol* 590:3349-60.
- 1456 Lee C, Zeng J, Drew BG, Sallam T, Martin-Montalvo A, Wan J, Kim SJ, Mehta H, Hevener AL, de Cabo R,  
1457 Cohen P (2015) The mitochondrial-derived peptide MOTS-c promotes metabolic homeostasis and reduces  
1458 obesity and insulin resistance. *Cell Metab* 21:443-54.
- 1459 Lee SR, Kim HK, Song IS, Youm J, Dizon LA, Jeong SH, Ko TH, Heo HJ, Ko KS, Rhee BD, Kim N, Han J  
1460 (2013) Glucocorticoids and their receptors: insights into specific roles in mitochondria. *Prog Biophys Mol*  
1461 *Biol* 112:44-54.
- 1462 Leek BT, Mudaliar SR, Henry R, Mathieu-Costello O, Richardson RS (2001) Effect of acute exercise on citrate  
1463 synthase activity in untrained and trained human skeletal muscle. *Am J Physiol Regul Integr Comp Physiol*  
1464 280:R441-7.
- 1465 Lemieux H, Blier PU, Gnaiger E (2017) Remodeling pathway control of mitochondrial respiratory capacity by  
1466 temperature in mouse heart: electron flow through the Q-junction in permeabilized fibers. *Sci Rep* 7:2840.

- 1467 Lenaz G, Tioli G, Falasca AI, Genova ML (2017) Respiratory supercomplexes in mitochondria. In: Mechanisms  
1468 of primary energy trasduction in biology. M Wikstrom (ed) Royal Society of Chemistry Publishing, London,  
1469 UK:296-337.
- 1470 Margulis L (1970) Origin of eukaryotic cells. New Haven: Yale University Press.
- 1471 Meinild Lundby AK, Jacobs RA, Gehrig S, de Leur J, Hauser M, Bonne TC, Flück D, Dandanell S, Kirk N,  
1472 Kaech A, Ziegler U, Larsen S, Lundby C (2018) Exercise training increases skeletal muscle mitochondrial  
1473 volume density by enlargement of existing mitochondria and not de novo biogenesis. *Acta Physiol* 222,  
1474 e12905.
- 1475 Menshikova EV, Ritov VB, Fairfull L, Ferrell RE, Kelley DE, Goodpaster BH (2006) Effects of exercise on  
1476 mitochondrial content and function in aging human skeletal muscle. *J Gerontol A Biol Sci Med Sci* 61:534-  
1477 40.
- 1478 Menshikova EV, Ritov VB, Ferrell RE, Azuma K, Goodpaster BH, Kelley DE (2007) Characteristics of skeletal  
1479 muscle mitochondrial biogenesis induced by moderate-intensity exercise and weight loss in obesity. *J Appl*  
1480 *Physiol* (1985) 103:21-7.
- 1481 Menshikova EV, Ritov VB, Toledo FG, Ferrell RE, Goodpaster BH, Kelley DE (2005) Effects of weight loss  
1482 and physical activity on skeletal muscle mitochondrial function in obesity. *Am J Physiol Endocrinol Metab*  
1483 288:E818-25.
- 1484 Miller GA (1991) The science of words. Scientific American Library New York:276 pp.
- 1485 Mitchell P (1961) Coupling of phosphorylation to electron and hydrogen transfer by a chemi-osmotic type of  
1486 mechanism. *Nature* 191:144-8.
- 1487 Mitchell P (2011) Chemiosmotic coupling in oxidative and photosynthetic phosphorylation. *Biochim Biophys*  
1488 *Acta Bioenergetics* 1807:1507-38.
- 1489 Mogensen M, Sahlin K, Fernström M, Glintborg D, Vind BF, Beck-Nielsen H, Højlund K (2007) Mitochondrial  
1490 respiration is decreased in skeletal muscle of patients with type 2 diabetes. *Diabetes* 56:1592-9.
- 1491 Mohr PJ, Phillips WD (2015) Dimensionless units in the SI. *Metrologia* 52:40-7.
- 1492 Moreno M, Giacco A, Di Munno C, Goglia F (2017) Direct and rapid effects of 3,5-diiodo-L-thyronine (T2).  
1493 *Mol Cell Endocrinol* 7207:30092-8.
- 1494 Morrow RM, Picard M, Derbeneva O, Leipzig J, McManus MJ, Gousspillou G, Barbat-Artigas S, Dos Santos C,  
1495 Hepple RT, Murdock DG, Wallace DC (2017) Mitochondrial energy deficiency leads to hyperproliferation of  
1496 skeletal muscle mitochondria and enhanced insulin sensitivity. *Proc Natl Acad Sci U S A* 114:2705-10.
- 1497 Murley A, Nunnari J (2016) The emerging network of mitochondria-organelle contacts. *Mol Cell* 61:648-53.
- 1498 National Academies of Sciences, Engineering, and Medicine (2018) International coordination for science data  
1499 infrastructure: Proceedings of a workshop—in brief. Washington, DC: The National Academies Press. doi:  
1500 <https://doi.org/10.17226/25015>.
- 1501 Paradies G, Paradies V, De Benedictis V, Ruggiero FM, Petrosillo G (2014) Functional role of cardiolipin in  
1502 mitochondrial bioenergetics. *Biochim Biophys Acta* 1837:408-17.
- 1503 Pesta D, Gnaiger E (2012) High-Resolution Respirometry. OXPHOS protocols for human cells and  
1504 permeabilized fibres from small biopsies of human muscle. *Methods Mol Biol* 810:25-58.
- 1505 Pesta D, Hoppel F, Macek C, Messner H, Faulhaber M, Kobel C, Parson W, Burtscher M, Schocke M, Gnaiger  
1506 E (2011) Similar qualitative and quantitative changes of mitochondrial respiration following strength and  
1507 endurance training in normoxia and hypoxia in sedentary humans. *Am J Physiol Regul Integr Comp Physiol*  
1508 301:R1078–87.
- 1509 Price TM, Dai Q (2015) The role of a mitochondrial progesterone receptor (PR-M) in progesterone action.  
1510 *Semin Reprod Med* 33:185-94.
- 1511 Puchowicz MA, Varnes ME, Cohen BH, Friedman NR, Kerr DS, Hoppel CL (2004) Oxidative phosphorylation  
1512 analysis: assessing the integrated functional activity of human skeletal muscle mitochondria – case studies.  
1513 *Mitochondrion* 4:377-85. Puntschart A, Claassen H, Jostarndt K, Hoppeler H, Billeter R (1995) mRNAs of  
1514 enzymes involved in energy metabolism and mtDNA are increased in endurance-trained athletes. *Am J*  
1515 *Physiol* 269:C619-25.
- 1516 Quiros PM, Mottis A, Auwerx J (2016) Mitonuclear communication in homeostasis and stress. *Nat Rev Mol*  
1517 *Cell Biol* 17:213-26.
- 1518 Reichmann H, Hoppeler H, Mathieu-Costello O, von Bergen F, Pette D (1985) Biochemical and ultrastructural  
1519 changes of skeletal muscle mitochondria after chronic electrical stimulation in rabbits. *Pflugers Arch* 404:1-  
1520 9.
- 1521 Renner K, Amberger A, Konwalinka G, Gnaiger E (2003) Changes of mitochondrial respiration, mitochondrial  
1522 content and cell size after induction of apoptosis in leukemia cells. *Biochim Biophys Acta* 1642:115-23.
- 1523 Rich P (2003) Chemiosmotic coupling: The cost of living. *Nature* 421:583.
- 1524 Rostovtseva TK, Sheldon KL, Hassanzadeh E, Monge C, Saks V, Bezrukov SM, Sackett DL (2008) Tubulin  
1525 binding blocks mitochondrial voltage-dependent anion channel and regulates respiration. *Proc Natl Acad Sci*  
1526 *USA* 105:18746-51.



- 1527 Rustin P, Parfait B, Chretien D, Bourgeron T, Djouadi F, Bastin J, Rötig A, Munnich A (1996) Fluxes of  
1528 nicotinamide adenine dinucleotides through mitochondrial membranes in human cultured cells. *J Biol Chem*  
1529 271:14785-90.
- 1530 Saks VA, Veksler VI, Kuznetsov AV, Kay L, Sikk P, Tiivel T, Tranqui L, Olivares J, Winkler K, Wiedemann F,  
1531 Kunz WS (1998) Permeabilised cell and skinned fiber techniques in studies of mitochondrial function in  
1532 vivo. *Mol Cell Biochem* 184:81-100.
- 1533 Salabei JK, Gibb AA, Hill BG (2014) Comprehensive measurement of respiratory activity in permeabilized cells  
1534 using extracellular flux analysis. *Nat Protoc* 9:421-38.
- 1535 Sazanov LA (2015) A giant molecular proton pump: structure and mechanism of respiratory complex I. *Nat Rev*  
1536 *Mol Cell Biol* 16:375-88.
- 1537 Schneider TD (2006) Claude Shannon: biologist. The founder of information theory used biology to formulate  
1538 the channel capacity. *IEEE Eng Med Biol Mag* 25:30-3.
- 1539 Schönfeld P, Dymkowska D, Wojtczak L (2009) Acyl-CoA-induced generation of reactive oxygen species in  
1540 mitochondrial preparations is due to the presence of peroxisomes. *Free Radic Biol Med* 47:503-9.
- 1541 Schultz J, Wiesner RJ (2000) Proliferation of mitochondria in chronically stimulated rabbit skeletal muscle--  
1542 transcription of mitochondrial genes and copy number of mitochondrial DNA. *J Bioenerg Biomembr* 32:627-  
1543 34.
- 1544 Simson P, Jepihhina N, Laasmaa M, Peterson P, Birkedal R, Vendelin M (2016) Restricted ADP movement in  
1545 cardiomyocytes: Cytosolic diffusion obstacles are complemented with a small number of open mitochondrial  
1546 voltage-dependent anion channels. *J Mol Cell Cardiol* 97:197-203.
- 1547 Stucki JW, Ineichen EA (1974) Energy dissipation by calcium recycling and the efficiency of calcium transport  
1548 in rat-liver mitochondria. *Eur J Biochem* 48:365-75.
- 1549 Tonkonogi M, Harris B, Sahlin K (1997) Increased activity of citrate synthase in human skeletal muscle after a  
1550 single bout of prolonged exercise. *Acta Physiol Scand* 161:435-6.
- 1551 Waczulikova I, Habodaszova D, Cagalinec M, Ferko M, Ulicna O, Mateasik A, Sikurova L, Ziegelhöffer A  
1552 (2007) Mitochondrial membrane fluidity, potential, and calcium transients in the myocardium from acute  
1553 diabetic rats. *Can J Physiol Pharmacol* 85:372-81.
- 1554 Wagner BA, Venkataraman S, Buettner GR (2011) The rate of oxygen utilization by cells. *Free Radic Biol Med*  
1555 51:700-712.
- 1556 Wang H, Hiatt WR, Barstow TJ, Brass EP (1999) Relationships between muscle mitochondrial DNA content,  
1557 mitochondrial enzyme activity and oxidative capacity in man: alterations with disease. *Eur J Appl Physiol*  
1558 *Occup Physiol* 80:22-7.
- 1559 Watt IN, Montgomery MG, Runswick MJ, Leslie AG, Walker JE (2010) Bioenergetic cost of making an  
1560 adenosine triphosphate molecule in animal mitochondria. *Proc Natl Acad Sci U S A* 107:16823-7.
- 1561 Weibel ER, Hoppeler H (2005) Exercise-induced maximal metabolic rate scales with muscle aerobic capacity. *J*  
1562 *Exp Biol* 208:1635-44.
- 1563 White DJ, Wolff JN, Pierson M, Gemmell NJ (2008) Revealing the hidden complexities of mtDNA inheritance.  
1564 *Mol Ecol* 17:4925-42.
- 1565 Wikström M, Hummer G (2012) Stoichiometry of proton translocation by respiratory complex I and its  
1566 mechanistic implications. *Proc Natl Acad Sci U S A* 109:4431-6.
- 1567 Willis WT, Jackman MR, Messer JI, Kuzmiak-Glancy S, Glancy B (2016) A simple hydraulic analog model of  
1568 oxidative phosphorylation. *Med Sci Sports Exerc* 48:990-1000.